JOURNAL OF GEOPHYSICAL RESEARCH, VOL. 95, NO. B6, PAGES 8357–8381, JUNE 10, 1990

Orogeny and Large-Scale Strike-Slip Faulting on Venus: Tectonic Evolution of Maxwell Montes

R.W. VORDER BRUEGGE AND J.W. HEAD

Department of Geological Sciences, Brown University, Providence, Rhode Island

D.B. CAMPBELL

National Astronomy and Ionosphere Center, Cornell University, Ithaca, New York

The Ishtar Terra highland region of Venus contains mountain belts morphologically similar to terrestrial orogenic belts. Akna Montes and Freyja Montes are long, linear mountain belts with about 4 km of relief above the 3- to 4-km-high Lakshmi Planum. The Maxwell Montes mountain belt, however, is more rectangular in plan view and has relief of approximately 8 km. We have investigated the nature of this latter range using complementary radar images obtained by the Arecibo Observatory and the Venera 15/16 spacecraft, as well as altimetry data obtained by the Venera 15/16 and Pioneer Venus spacecraft. Geological and structural maps have been compiled on the basis of these data, the individual features and their stratigraphic relationships interpreted, and a model for the origin and evolution of Maxwell Montes is proposed. The dominant features of this mountain range are long, parallel ridges and valleys that are intepreted to be anticlines and synclines and to have resulted from ENE-WSW oriented compression. Two major shear zones bound Maxwell Montes on the north and south, converging toward the west. Nine narrow linear parallel features several hundreds of kilometers long (identified as cross-strike discontinuities, CSDs) cut obliquely across the strike of the ridges and valleys in a NW-SE direction and disrupt the structural fabric of the mountain range, dividing Maxwell Montes into 10 crustal domains. Among several possible origins, we find that the data are most consistent with their interpretation as right-lateral strike-slip faults with offsets of up to 125 km. Retrodeformation and reconstruction of Maxwell Montes using the offsets determined for individual domains produces a long linear mountain range similar to Akna Montes. Using geologic unit maps and topographic maps of the present configuration of Maxwell, similar reconstructions were made; these reconstructions restored several linear tectonic elements, topographic trends, and sinuous unit boundaries to more contiguous positions. On the basis of these data and observations we suggest that Akna Montes may represent the initial form of compressional orogenic belts on Venus, while Maxwell Montes attained its present morphology through a second stage of deformation involving large-scale strike-slip faulting. We examine several models for this second stage and favor the interpretation that it occurred as the Akna Montes-like proto-Maxwell Montes was transported to the west between two converging shear zones, accompanied by rotation of the entire mountain range. Thirty percent shortening of the mountain range is implied by the geometries of the present and reconstructed Maxwell Montes. On the basis of the deformation in Maxwell Montes and the evidence for large-scale transport we conclude that large-scale horizontal movement of crustal materials is a significant aspect of the tectonics of Venus.

INTRODUCTION

The global tectonic style of Venus has yet to be defined. However, mountain belts which are morphologically and topographically similar to orogenic belts on Earth have been observed on Venus [*Masursky et al.*, 1980; *Campbell et al.*, 1983; *Barsukov et al.*, 1986]. Two of these mountain belts, Akna Montes and Freyja Montes, have previously been interpreted as orogenic belts based on the recognition of a number of diagnostic features analogous to those observed in terrestrial orogenic belts [*Crumpler et al.*, 1986]. A third mountain belt, Maxwell Montes, is the focus of this study. We present evidence that this range was initially formed compressionally as an Akna Montes-like linear mountain belt and that it experienced a later stage of large-scale strike-slip faulting accompanied by 30% shortening parallel to its long axis. We conclude that large-scale horizontal movement of crustal materials has been an intrinsic part of the tectonics of Venus.

Paper number 89JB03628.
0148-0227/90/89JB-03628$05.00

DATA SETS AND APPROACH

Our investigation involved a comparative analysis of radar images and altimetry from several sources. Images analyzed include those obtained by the Arecibo Observatory (Figure 1*a*) and the Venera 15 and 16 spacecraft (Figure 1*b*), both of which have spatial resolution in the range of 1-2 km. We have also used altimetry obtained by the Pioneer Venus orbiter (Figure 1*c*) and the Venera 15/16 orbiters (Figure 2*c*). The Pioneer Venus altimetry has a vertical accuracy of approximately 200 m, and footprint sizes for the area of interest are typically about 50 km by 50 km [*Pettengill et al.*, 1980]. The Venera altimetry has a precision of 50 m and footprint diameters of 40-50 km [*Rzhiga*, 1987].

The Arecibo and Venera 15/16 imaging radar systems provide complementary coverage of the Maxwell Montes area due to their differing look directions and incidence angles. The Arecibo system illuminated Maxwell Montes from the southwest at incidence angles between 59° and 65°, whereas the Venera system illuminated Maxwell from the east at incidence angles between 7° and 13°. From the scattering law of *Hagfors* [1964, 1970] it is predicted that at the given incidence angles, the Arecibo system is most sensitive to variations in small-scale (centimeter-meter) surface roughness and intrinsic

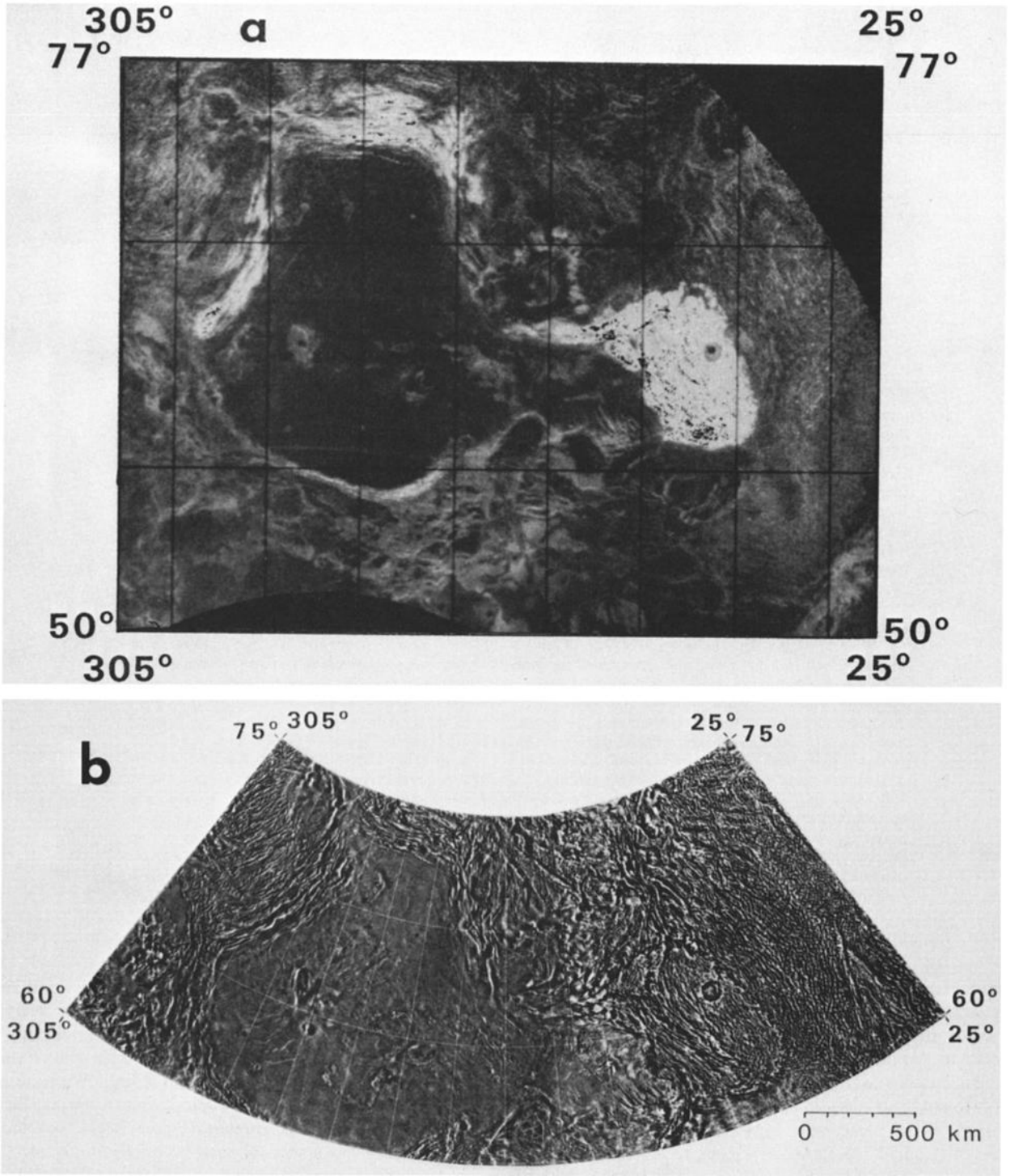

Fig. 1. Western and central Ishtar Terra. Width of this region is approximately 3500 km. The 3- to 4-km-high plateau, Lakshmi Planum, is flanked to the west, north, and east by the Akna Montes, Freyja Montes, and Maxwell Montes mountain belts, respectively. (*a*) Mercator projection of Arecibo mosaic of Ishtar Terra. (*b*) Lambert equal-area projection of Venera mosaic of Ishtar Terra. (*c*) Pioneer Venus topography of Ishtar Terra. Contour interval is 500 m from a base level of 6051.4 km.

reflectivity, whereas the Venera system is most sensitive to variations in longer-wavelength surface slopes. Therefore, in Arecibo images, rough and/or high-reflectivity materials appear bright, whereas smooth and/or low-reflectivity materials appear dark. In Venera images, east facing slopes appear bright and west facing slopes appear dark. The differences resulting from these geometries make these data sets complementary in the sense that differing aspects of surface properties and morphology are determined for the same area, as is evident in Figures 1*a* and 1*b*.

In this paper we use these complementary data sets to produce geologic and structural maps of Maxwell Montes and use the results to compare its characteristics to the other linear mountain belts. We then assess the tectonic deformation

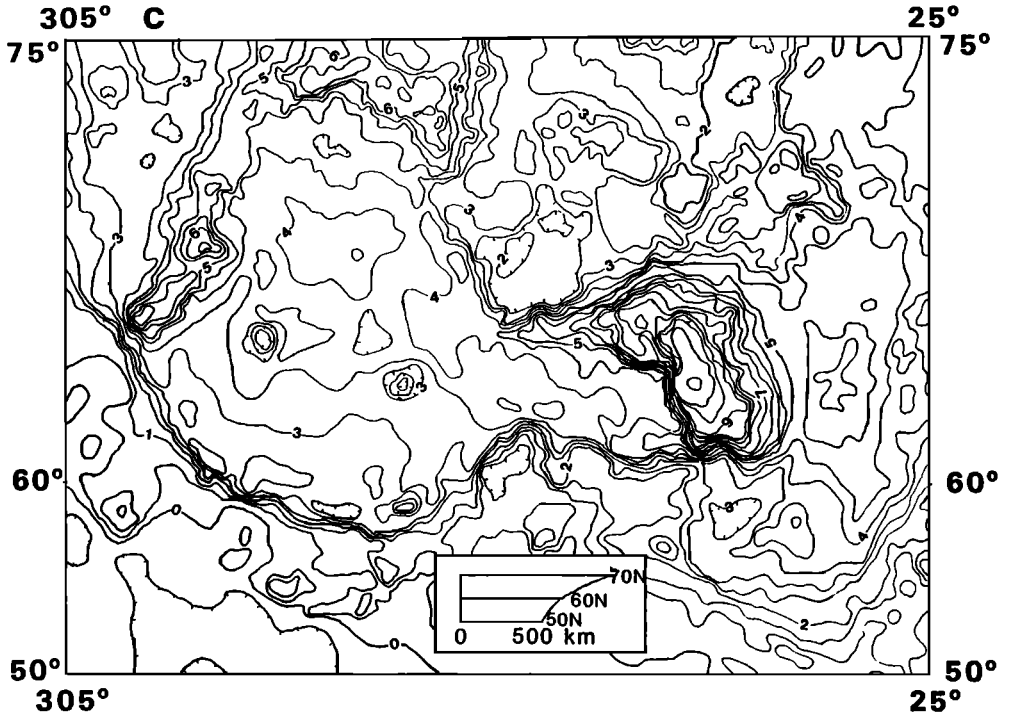

Fig. 1. (continued)

occurring there, identifying the structural elements, their tectonic origin, and their sequence. Finally, we develop a geologic and tectonic chronology and propose a model for the origin and evolution of Maxwell Montes.

Regional Description, Surface Morphology, and Geologic Mapping

The Ishtar Terra Highland region on Venus (Figure 1) is dominated by the plateau Lakshmi Planum, which is elevated 3-4 km above the surrounding plains and which is surrounded by linear mountain belts [*Masursky et al.*, 1980; *Campbell et al.*, 1983; *Barsukov et al.*, 1986; *Basilevsky et al.*, 1986]. These mountain belts are from 200 to 500 km wide, extend to over 1000 km in length, and possess 3-8 km of relief relative to the plateau. The belts on the western and northern flanks of Lakshmi Planum, Akna Montes and Freyja Montes (Figure 1), are morphologically similar to terrestrial orogenic belts [*Crumpler et al.*, 1986]. In contrast, Maxwell Montes is far more rectilinear in plan view and possesses twice the relief of the other mountain belts. The most distinctive characteristic of Maxwell Montes in the Arecibo image (Figure 2*a*) is its high radar backscatter cross section relative to the surrounding terrain. The boundary defining the area of high backscatter cross section closely follows the 6-km altitude contour (Figure 2*c*).

In both data sets, the most distinctive features of Maxwell Montes and the other linear mountain belts are paired, parallel bright and dark bands (Figures 1 and 2). These bands represent topographic ridges and valleys in the Venera 15/16 image and relatively rough and smooth areas in the Arecibo image. Uncertainties in the kilometer-scale topography of this region precludes a direct correlation of individual ridge/valley and rough/smooth pairs across the mountain range, but we find that there are broad areas where the ridges observed in the Venera data correspond well with the rough areas observed in the Arecibo data. Therefore we conclude that the ridge crests on Maxwell Montes are characterized by relatively rough surfaces, while the valleys are characterized by relatively smooth surfaces. If erosion rates are low on Venus, as suggested from surface lander images [*Garvin et al.*, 1984] and reflectivity data [*Pettengill et al.*, 1982], then the crests of the ridges may be rough simply due to tectonic breakup of ridge crests and concentration of rock debris not far from the crests. The troughs, however, could be smoother due to collection of soil in lows or a lack of tectonic breakup and concentration of talus on the ridge and its flanks. In addition to these rough, linear ridges and smooth valleys, there are also areas of shorter bright ridges that are parallel or intersect one another at a variety of angles. Some ridges are also observed that are more sigmoidal in shape. Finally, other features that are recognized as individual bright or dark linear segments are observed in the images. These features are interpreted to represent scarps, faults, or fractures, and their occurrence is far less frequent than that of the parallel ridges and troughs.

Continuous areas of similar structures and textures can be identified across Maxwell Montes and mapped as geomorphic and geologic units. The key factors in identifying particular units are a similarity in structures, texture, and overall backscatter cross section. Through a comparison of the Arecibo and Venera images, 10 distinctive morphologies can be recognized across Maxwell Montes, identified as units, and compiled in a geological map (Figure 2*d*). A detailed description of each of these units is provided elsewhere [*Vorder Bruegge*, 1987], but similarities in the features and textures of some units enable us to define four basic groupings of units (Figure 2*d*). We interpret the nature and origin of these units based on their structures, textures, locations, and correspondence to the detailed topography (Figure 2*c*).

The "Banded Units" are composed predominantly of long,

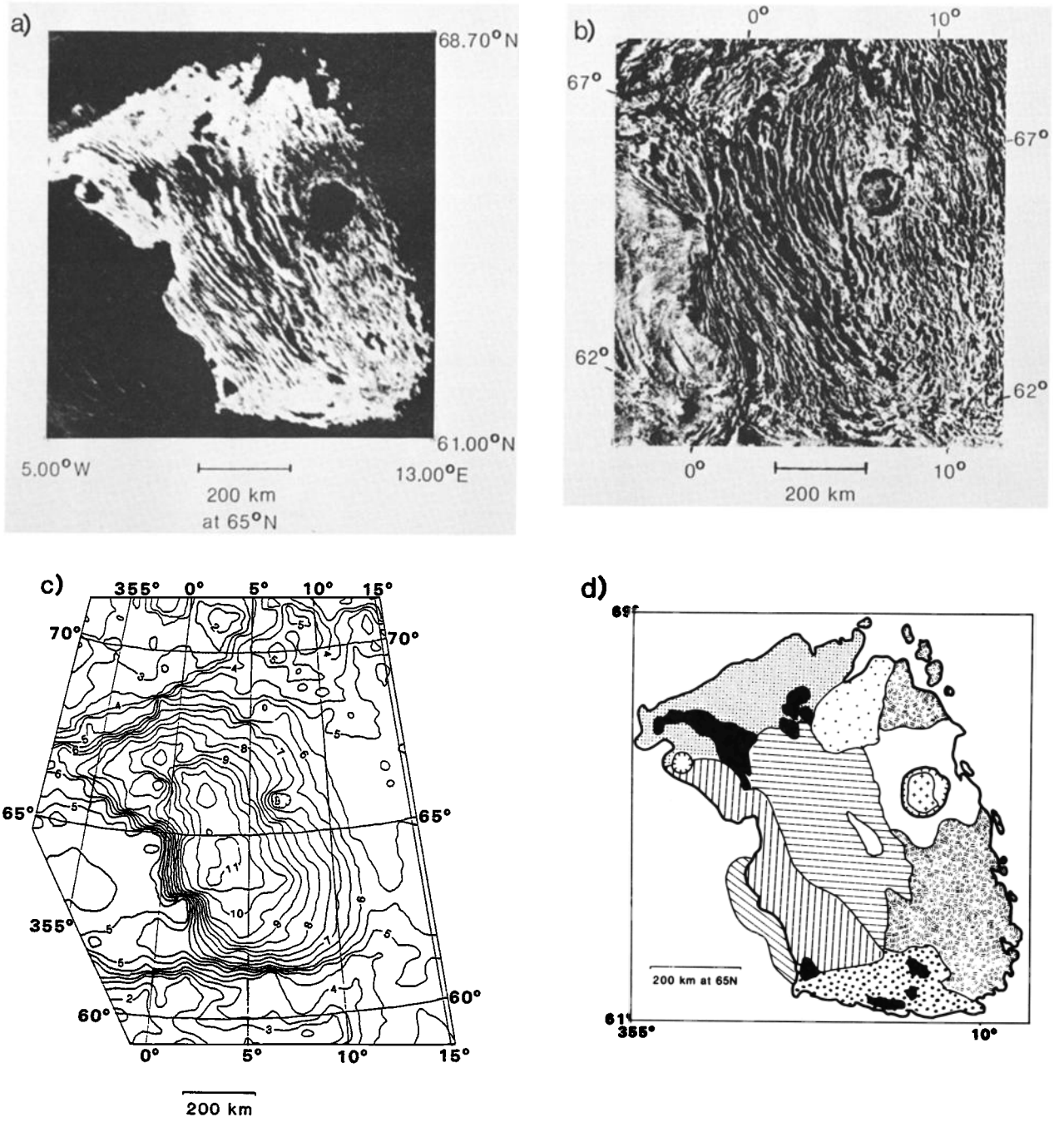

Fig. 2. Maxwell Montes and surrounding areas. (*a*) Arecibo image of Maxwell Montes, Mercator projection. (*b*) Lambert equal area projection of Venera mosaic of Maxwell Montes. (*c*) Venera topography of Maxwell Montes area. Contour interval is 500 m from a base level of 6051.0 km. (*d*) Geological unit map of Maxwell Montes, derived from comparison of Arecibo and Venera data sets. Detailed descriptions of individual units are given elsewhere [*Vorder Bruegge*, 1987]. Unit groupings are defined in text.

linear, parallel ridges and valleys. These features are oriented parallel to the strike of the mountain belt, and the units occur along the steep western slope and along the crest of the mountain range (Figure 2). Most workers have interpreted these ridges and valleys as compressional features based on a number of observations and arguments including: (1) the continuous nature and regular spacing of ridges [*Campbell et al.*, 1983; *Burke et al.*, 1984; *Solomon and Head*, 1984]; (2) evidence of fold closure of some ridges [*Burke et al.*, 1984]; and (3) the morphological similarity of ridges and valleys in Maxwell to those in the Akna and Freyja orogenic belts, which were interpreted as compressional on the basis of several characteristics including symmetry of the ridges and troughs, suggesting that these represent anticline-syncline pairs; broad, low arches similar to mare-ridge-type features seen on the Moon and interpreted to represent low-angle thrusting and buckling; and linear discontinuities that cut across the strike of the ridges and troughs and are interpreted to represent strike-slip movement [*Crumpler et al.*, 1986]. All of these observations and the overall similarity of ridges on Maxwell to those on Akna and Freyja lead us to interpret them as compressional anticlines and synclines. The strike of the majority of ridges in Maxwell as well as the strike of the mountain belt is approximately N20°W, implying a maximum principal stress axis oriented N70°E.

The "complex unit" (the "dissected terrain") occurs on the gentle eastern slope of Maxwell Montes (Figure 2). In this unit, very short ridge segments abruptly terminate or are intersected by other ridge segments. This unit has a high overall backscatter cross section, suggesting that rough materials occur pervasively. The NNW-SSE dominant trend of ridges in this unit, and their parallelism to the bands in the adjacent banded units is consistent with a compressional origin, with compression oriented along a ENE-WSW axis similar to that seen in the banded units. Although we interpret the ridges to be of a regional compressional origin, the dissected and intersecting nature of many of the ridges and the overall roughness suggests greater tectonic deformation than in the banded units, perhaps resulting from an additional episode not related to the ENE-WSW compression or due to a different mechanical response in eastern Maxwell. A similar type of terrain has been recognized in the Freyja Montes region of northern Ishtar Terra [*Head*, 1990]. Identified as the "ridged and domed unit," this terrain extends down the gentle backslope of Freyja Montes, out across a broad plateau, and is characterized by linear hills, swales, and equidimensional domelike features [*Head*, 1990]. As in Maxwell Montes, the predominant trend of the linear ridges in the ridged and domed unit parallels that of the ridges in the adjacent banded unit of Freyja Montes, all of which are interpreted to have a compressional origin [*Head*, 1990].

The "transitional units" occur on the steep northern and southern slopes of Maxwell, and contain intermediate-length ridge segments which are typically aligned with the NNW trending ridges of the banded units and the dissected terrain. These ridges are also interpreted to be of regional compressional origin, but they are not as continuous as those in the banded units and are commonly arcuate and occur in anastomosing or braided patterns. Occasionally, linear troughs and/or ridges disrupt the continuity of, and strike perpendicular to, the NNW trending ridges. As in the dissected unit, these units are distinguished by their relatively high radar backscatter cross section, suggesting the pervasiveness of rough materials. The relatively great roughness of these units may be attributed to the steep regional slopes which would favor downslope movement of talus throughout these units. More likely, the relatively great roughness is due to regional deformation associated with north and south bounding shear zones identified in previous studies [*Basilevsky et al.*, 1986; *Pronin et al.*, 1986; *Head*, 1986] and discussed below. Relative motion along these shear zones might result in some parallel faulting and additional deformation on Maxwell Montes, leading to increased roughness. Linear troughs oriented perpendicular to the NNW trending ridges on the northern and southern slopes of Maxwell (Figure 2*b*) may represent such faults. Alternatively, these linear troughs could be related to gravitational effects such as gravity sliding or large-scale relaxation.

The "smooth units" are all characterized by homogeneous texture and a lack of kilometer-scale structures. They have a lower backscatter cross section than the rest of Maxwell Montes, indicative of less small-scale roughness and lower reflectivity. Large smooth areas associated with the circular feature Cleopatra occur on a gentle slope, and appear to embay or bury ridges in the surrounding areas (Figure 2). These deposits do not appear to have been deformed by the same events that produced the surrounding ridges, suggesting that they were emplaced following the ridge-forming deformation. They have been interpreted as volcanic flows originating from Cleopatra Patera [*Schaber et al.*, 1987*a*], but they could also represent impact ejecta or impact melt from Cleopatra [*Ivanov et al.*, 1986]. The high backscatter cross section of these deposits relative to the rest of the planet is consistent with the interpretation that they represent impact ejecta since impact craters on Venus often have radar-bright ejecta blankets [*Basilevsky et al.*, 1987]. In addition, some of this "bright terrain" is presently observed upslope from Cleopatra to the west (Figure 2), an observation that also might tend to favor an impact origin. However, caution is also required in this interpretation since some uplift to the west of Cleopatra may have occurred after the emplacement of the bright terrain. The other smooth units (Figure 2*d*) occur in isolated patches across Maxwell Montes in local lows. These local lows occur close to the 6-km altitude contour, and since areas below 6 km near Maxwell Montes are generally radar-dark, then these isolated patches may be radar-dark because they also occur below the 6-km contour and are being affected by the same process that makes other sub-6-km areas radar dark. Alternatively, the low backscatter cross section of these patches indicates that they are relatively smooth materials, inconsistent with large accumulations of talus. This observation, when coupled with the apparent lack of large-scale erosion on Venus mentioned above [*Garvin et al.*, 1984; *Pettengill et al.*, 1982], suggests that these patches could represent accumulations of volcanic materials, rather than talus or soil deposits.

The identification of smooth units west and south of Maxwell Montes as volcanic flows has been well established based on their embayment relationships, their flatness, uniform radar backscatter, and their association with volcanic source vents [*Basilevsky et al.*, 1986; *Pronin et al.*, 1986; *Magee and Head*, 1988]. These flows embay some ridges off the southern slope of Maxwell, but in contrast to the smooth units there is some evidence that these volcanic plains have undergone some tectonic deformation. In particular, immediately west of Maxwell Montes is a unit we identify as "dark ridges" (Figure 2). The structure and strike of these ridges

observed in the Venera image (Figure 2*b*) are almost identical to those of ridges in the adjacent banded units on Maxwell Montes, so they are also interpreted to be compressional in origin. However, two observations distinguish these ridges from others on Maxwell Montes: (1) The dark ridges unit is located on a relatively flat plain at 4-5 km elevation, in contrast to the steep relief associated with ridge units on Maxwell; and (2) the roughness and reflectivity of this unit (Figure 2*a*) more closely resemble those of the adjacent plains units than they do the banded units on Maxwell. The similarity in backscatter between the dark ridges and the Lakshmi plains units can be attributed to the formation of these ridges through the folding and thrusting of the volcanic plains materials, and the lack of large-scale relief associated with these ridges (unlike on Maxwell) indicates that they probably have accommodated minimal strain with little crustal thickening.

Additional tectonic deformation of the smooth plains in Lakshmi is observed to the southwest of Maxwell Montes in the form of long, arcuate troughs which *Ronca and Basilevsky* [1986] identified as extensional "joints." These troughs are not embayed by plains materials but appear to disrupt them. While *Ronca and Basilevsky* [1986] attributed these features to extension associated with motion along a shear zone south of Maxwell, an alternative explanation is that these fossae represent extension due to loading and flexure associated with the mass of Maxwell Montes. However, if loading and flexure were responsible for these chasmata, then one might expect them to be present all around Maxwell. Since these features are not observed elsewhere, we favor the interpretation that they are associated with relative motion along that shear zone. Whatever their origin, their disruption of the plains unit indicates that they are relatively younger than the plains.

The style of deformation in the various units and their distribution in and around Maxwell Montes provides some insight into the processes affecting the mountain range as a whole. The ridges and valleys of the banded units in western Maxwell Montes result from compressional deformation along a N70°E axis, as do the ridges and valleys in the dissected terrain unit to the east. *Head* [1990] has described a similar pattern in Freyja Montes, with a banded unit and an adjacent ridged and domed unit also interpreted as resulting from compressional deformation. The increased roughness and disruption in the dissected terrain (and likewise in the ridged and domed unit) suggest further deformation affecting this region and possibly involving faulting, transpression, and tectonic segmentation that may not necessarily be associated with the primary compressional phase. The "transitional units" may have been affected by gravitational influences and interaction with the north and south bounding shear zones, in addition to the compressional phase. Finally, the relatively low backscatter cross section of some of the smooth units and their correspondence to local lows suggests that these units may represent volcanic flows or impact ejecta and melt. Their lack of deformation indicates that they were not subjected to the compressional deformation that disrupted the surrounding units and thus postdate the tectonic events.

Interpretation of Maxwell Montes as an orogenic belt. We interpret the large-scale configuration of Maxwell Montes in the unit map and topography (Figure 2) to be the result of east-west convergence of crustal materials accompanied by crustal thickening through processes of folding, thrusting, and buckling. This deformation is best characterized by the NNW trending ridges and valleys across central Maxwell Montes. A similar pattern characterizes the Akna and Freyja Montes orogenic belts [*Campbell et al.*, 1983; *Crumpler et al.*, 1986; *Head*, 1990], but the steep northern and southern flanks of Maxwell exhibit patterns of deformation not observed in the other orogenic belts. In particular, a simple model of east-west convergence cannot account for the complex deformation in the transitional units. Further deformation involving either gravitational effects along the steep slopes or interaction with shear zones in these regions must be responsible for the observed morphology.

On Earth, linear mountain belts with great relief are often characterized not only by compressional features, but extensional ones as well [*Molnar and Tapponnier*, 1978; *Dalmayrac and Molnar*, 1981; *Burchfiel and Royden*, 1985; *Armijo et al.*, 1986]. The great relief of these mountain belts leads to gravitational relaxation, which generally takes the form of normal faulting. Some of these normal faults strike parallel to the compressional features, often reactivating former thrust faults as extensional features [*Dalmayrac and Molnar*, 1981; *Burchfiel and Royden*, 1985], while other normal faults strike perpendicular to compressional features, parallel to the axis of maximum principal stress [*Molnar and Tapponnier*, 1978; *Armijo et al.*, 1986]. Although the former type of normal fault is often difficult to recognize in the field, the latter features often form fault-bounded graben that are easily identified from orbit [*Molnar and Tapponier*, 1978]. The resolution of the Arecibo and Venera data sets will not permit recognition of fold-parallel normal faulting along reactivated thrust faults such as those observed in the Himalaya only after considerable field work [*Burchfiel and Royden*, 1985]. However, fold-perpendicular graben with widths that exceed the spatial resolution of the Venera and Arecibo data should be recognizable if present. There is no obvious evidence of extensional graben formation perpendicular to the ridges or the strike of the mountain range in the banded units, although some such features may be present in the form of troughs in the transitional units as discussed above. The lack of obvious extensional features in central Maxwell, the highest region on the planet, and the potentially minimal extension represented by the troughs on the north and south slopes suggests that Maxwell Montes has not yet undergone extensive large-scale gravitational relaxation perpendicular to its strike.

Age of Maxwell Montes. The high surface temperature on Venus should make gravitational relaxation of high topography an important factor in the creation of tectonic features there [*Weertman*, 1979], and recent studies of Tellus Regio have supported this hypothesis [Bindschadler, D.L., et al., unpublished manuscript, 1989]. The time scales for such gravitational relaxation should be relatively short, leading to the relatively rapid removal of topographic relief [*Solomon et al.*, 1982]. The lack of impact craters in the Maxwell Montes region (with the possible exception of Cleopatra), and Venus as a whole, also attests to the relative youth of this region in comparison to the smaller terrestrial planets [*Basilevsky et al.*, 1986; *Schaber et al.*, 1987*b*]. In terms of absolute time, *Stephens et al.* [1983] predict that if only gravity acts on Maxwell Montes through a process of viscous relaxation, then the relief of Maxwell Montes will be removed in less than 1 b.y. Using this same model and assuming that Maxwell Montes may be relaxed today from even greater relief, *Stephens et al.* [1983] find that Maxwell Montes must be less than 200-600 m.y. old, making it a very recent geological event. However, the lack of evidence for large-scale gravitational relaxation in

the form of fold-perpendicular graben at the crest of Maxwell Montes suggests two things: (1) Maxwell Montes may be even younger than 200-600 m.y.; or (2) some dynamic process is inhibiting Maxwell Montes from undergoing gravitational relaxation, indicating that Maxwell Montes is active today or was active until very recently. In order to characterize better the tectonic activity and sequence of events of Maxwell Montes, we have examined the structural relationships within the mountain belt in greater detail.

STRUCTURAL MAPPING

Detailed structural mapping of Maxwell Montes using both the Arecibo and Venera imaging shows two major classes of structures: (1) the ridges and valleys which dominate the texture of the range, and (2) linear discontinuities which cut across the ridges and valleys.

Ridge and valley structure. We consider ridge/valley pairs as single structures because they are characterized in the radar images by paired bright and dark linear segments. In the Venera image, such a ridge is recognized as a radar-bright, east facing slope paired with a radar-dark, west facing slope to the immediate west. The point at which the radar-bright, east facing slope changes to a radar-dark, west facing slope is considered to be the crest of the ridge.

In the Arecibo image, we have already interpreted the radar-bright areas to be roughness associated with ridge crests. However, these radar-bright areas can be up to 10 km across, so that the specific location of a ridge crest within a radar-bright area is not immediately recognized. Examination of numerous digital number (DN or radar brightness) profiles perpendicular to prominant ridges in Maxwell Montes reveals that the most prominant ridges on Maxwell are broadly symmetrical about their peak brightness. This observation indicates that the roughness associated with prominant ridges on Maxwell Montes is symmetrically distributed about crests which exhibit peak roughness. From this we infer that the most distinctive ridges on Maxwell Montes are broadly symmetrical about the ridge crests. In Freyja Montes the ridges run parallel to the Venera radar look direction and this favorable geometry enabled *Crumpler et al.* [1986] to interpret the Freyja ridges as symmetrical anticlines. Since the ridges in Maxwell are otherwise morphologically similar to the symmetrical anticlines in Freyja Montes [*Crumpler et al.*, 1986] and based on their symmetry in DN profiles, we interpret the ridges to be symmetrical anticlines and the centers of these radar-bright areas to be the ridge crests. Since we have determined the ridge crests differently in the two data sets and because of uncertainties in coregistering the Arecibo and Venera images, we have mapped ridge crests separately for each of these data sets (Figure 3*a*).

Ridges are mapped as continuous features (Figure 3*a*) unless interrupted by one of the following: (1) Ridge termination such that the bright-dark pair identified as a single ridge is no longer discernable (this most commonly occurs as a bright ridge segment adjacent to a dark feature or area along strike); (2) an abrupt change in the width of the ridge of 50% or more (over less than 5 km); (3) an abrupt change in ridge-strike of 15° or more (over less than 5 km); or (4) any combination of these changes. Using these criteria, the mapping in Figure 3*a* shows the ridges to be extremely discontinuous along strike, with over 1000 ridge segments mapped in both the Arecibo and Venera data sets (Table 1). Individual ridge segments had a minimum length of 8 km and a maximum length of 80 km, with an average length of approximately 16 km in both data sets (Table 1).

Ford [1980] found that linear features aligned perpendicular to the radar look direction tend to be enhanced while features aligned parallel to the look direction tend to be subdued. In order to test this effect and to quantify the orientation of ridges on Maxwell Montes we have plotted rose diagrams of ridge frequency and length in 10° bins in Figure 4. The look directions of the Arecibo and Venera systems for Maxwell Montes are approximately N45°E and N85°E. Figure 4 reveals an overall agreement between the two data sets with the majority of ridges striking between N20°W and N40°W, parallelling the general strike of the mountain topography to the NNW (Figure 2). The minimal number of ridges observed parallel to both the Arecibo and Venera look directions in both data sets indicates that ridges are not being subdued there and that the ridge distributions mapped in Figure 3 are not biased

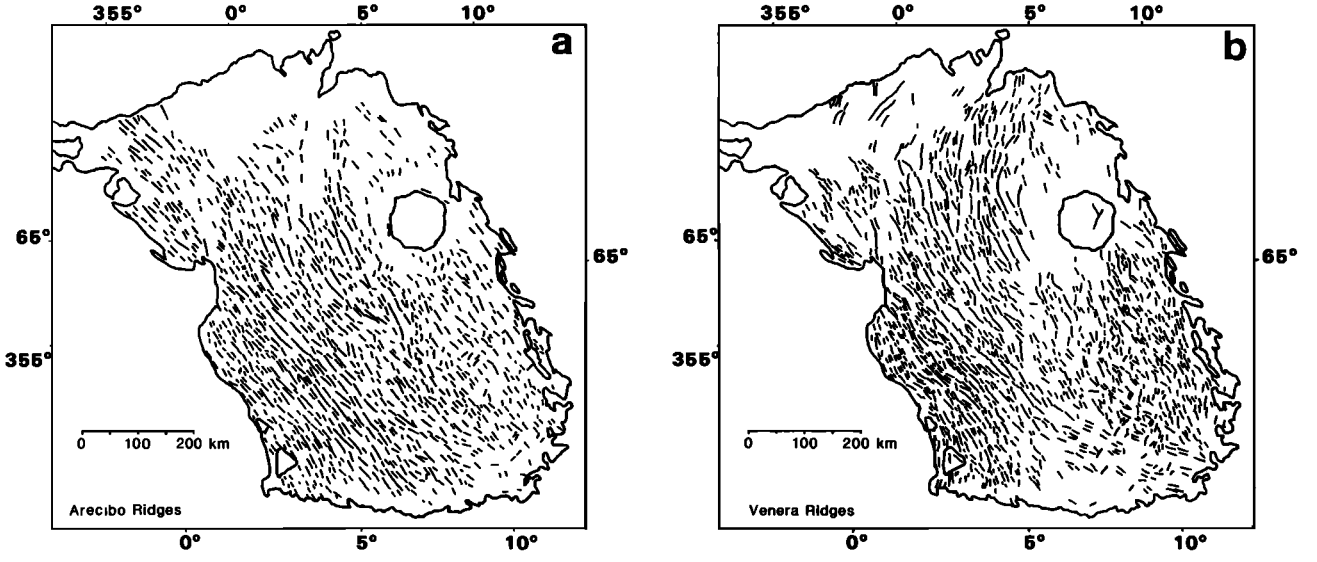

Fig. 3. Structural mapping of Maxwell Montes. The outline represents the high radar backscatter cross section boundary of Maxwell Montes. (*a*) Arecibo ridge map. (*b*) Venera ridge map. Solid lines represent interpreted crests of individual ridges.

TABLE 1. Ridge Statistics

Radar System	Number of Ridges	Total Ridge Length, km	Average Ridge Length, km
Venera	1265	20,124	15.91
Arecibo	1041	16,268	15.63

by the viewing geometry. We suggest that this is due to the fact that the ridges have a measurable width and are too large to be affected by look direction bias.

Linear discontinuities. The second type of feature mapped are individual linear discontinuities (Figure 5) which disrupt the structural trends defined by the ridges and troughs. Their distribution is shown in Figure 6. They are most often recognized by the termination of ridges against them, and they sometimes intersect and cross one another. These lineaments are always less than 5 km wide and can be 100 km in length or

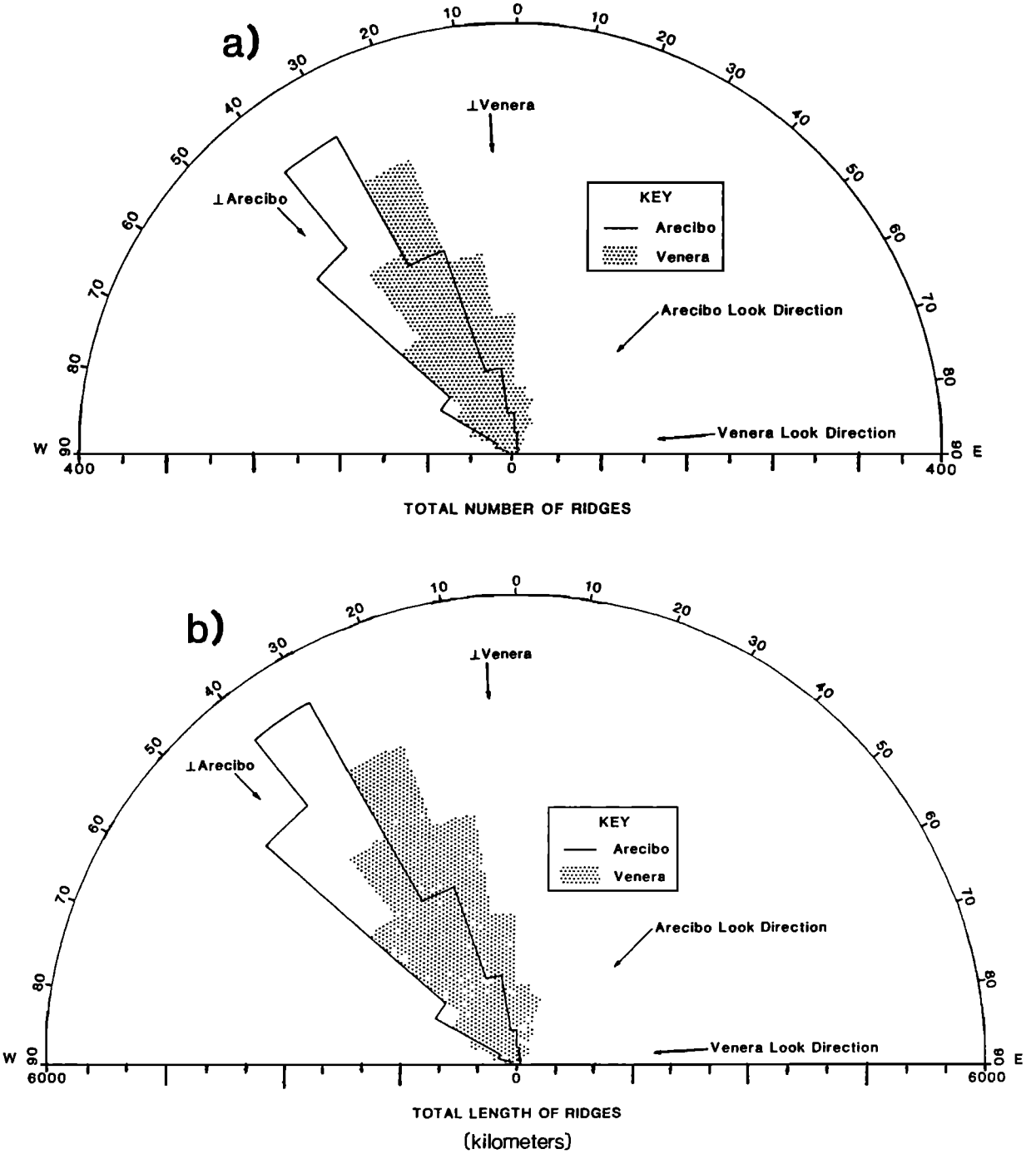

Fig. 4. Rose diagrams of Arecibo (outlined) and Venera (stippled) ridges. Bin size is 10°. (*a*) Total number of ridges. (*b*) Total length of ridges. Note look directions.

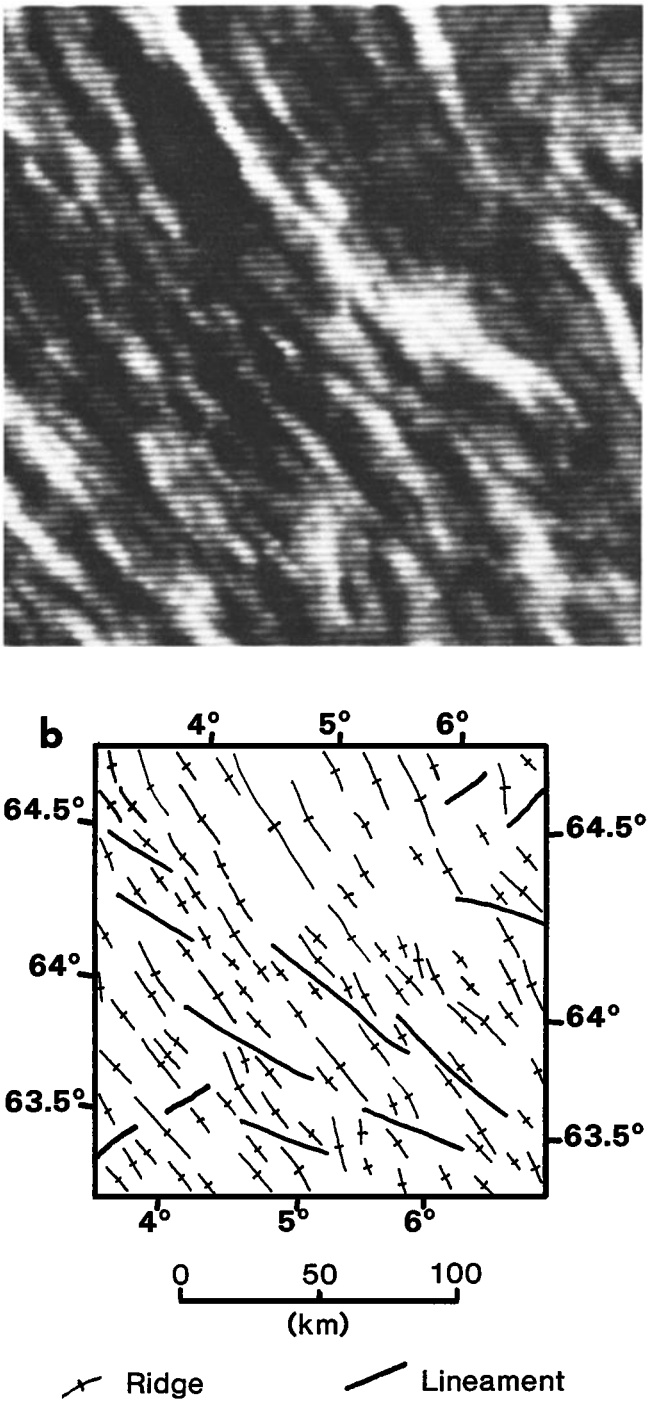

Fig. 5. Lineament example (*a*) Arecibo locator map. (*b*) Sketch map showing ridges (hatched lines) and lineaments (solid lines).

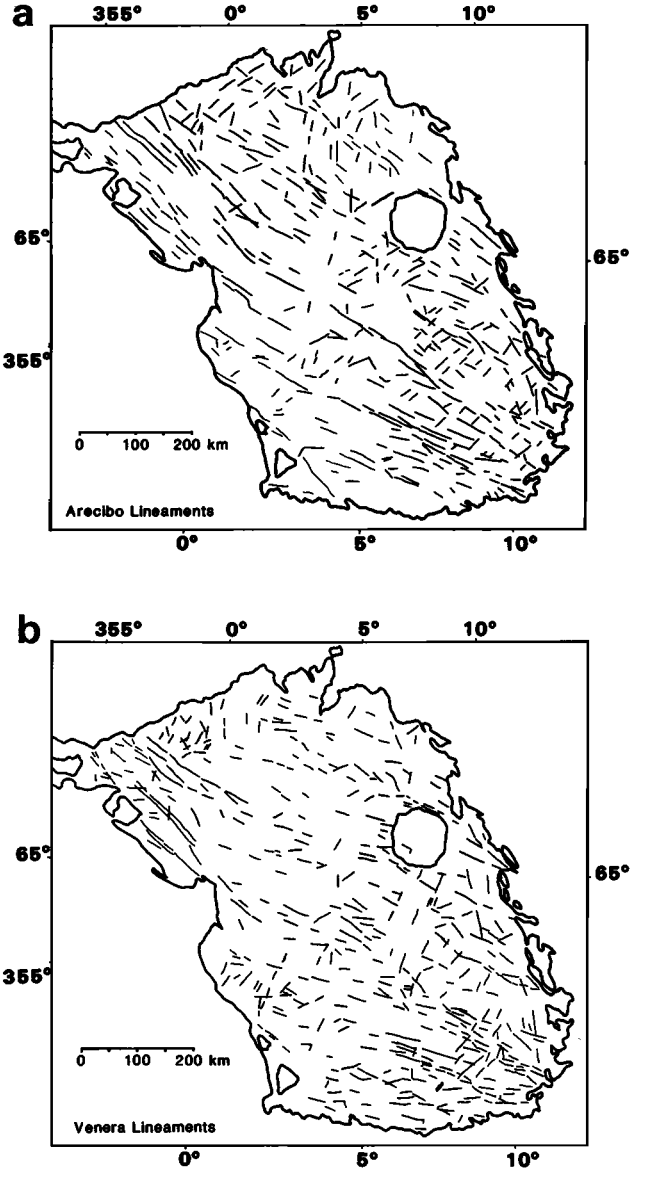

Fig. 6. (*a*) Arecibo lineament map. (*b*) Venera lineament map.

more. They can be bright or dark in either data set and could therefore represent faults, fractures, scarps, or ridges and troughs which are too small to be completely resolved by the radar systems. In particular, in the Venera data, a bright lineament most likely represents an east facing scarp or a small ridge at the limit of resolution, while a dark lineament might represent a west facing scarp or fault. Dark lineaments in the Arecibo data most likely represent faults or smooth scarps, while bright lineaments could represent rough ridges at the limit of resolution or faults filled with rough material.

The majority of the lineaments in both data sets are dark, an observation that may be due to the fact that dark features are more easily seen when they interrupt the continuity of the bright ridge structures. This also helps explain why these lineaments terminate most often in radar-dark areas, such as the smooth valleys in the Arecibo data and the west facing slopes in the Venera data, where they become indistinguishable from their surroundings. Resolved lineaments have a minimum length of 8 km and a maximum length of 140 km. More than 400 lineaments have been mapped with an average length of 24 km in both data sets (Table 2). The rose diagrams of Figure 7 reflect a dominant orientation of lineaments between N50°W and N80°W in both data sets. It is interesting to note that this major concentration of lineaments is close to perpendicular to the Arecibo look direction and close to parallel to the Venera look direction (Figure 7). This may account for the greater number and length of lineaments in the Arecibo data between N50°W and N70°W. The occurrence of a great number of lineaments within this range in the Venera data (Figure 7)

TABLE 2. Lineament Statistics

Radar System	Number of Lineaments	Total Lineament Length, km	Average Lineament Length, km
Venera	470	11157	23.74
Arecibo	410	9915	24.18

confirms that there actually are many lineaments in this orientation, and that the Arecibo look direction enhances their detection.

Cross-strike discontinuities. Close examination of the lineament maps of Figure 6 reveals that some of the longest lineaments are aligned with one another to form several semicontinuous, subparallel, linear features across the entire width of Maxwell Montes. The dominant trend of these semicontinuous linear features is between N50°W and N60°W, matching the dominant trend of the individual lineaments (Figure 7). In addition, further examination of the ridge maps (Figure 3) reveals that individual ridge discontinuities occur along the trend of the semicontinuous linear features, in the gaps between individual lineament segments. As described above, discontinuities in ridges can take the form of ridge termination, changes in ridge strike, changes in ridge width, or combinations of these. When these individual lineaments and ridge discontinuities are combined, they define nine subparallel, linear features that trend approximately N55°W and are generally continuous across the entire mountain belt. Since these linear features cut across the strike of the ridges and valleys on Maxwell Montes we refer to them as cross-strike discontinuities or CSDs after *Wheeler* [1980]. The individual lineaments and ridge discontinuities used to identify the CSDs are mapped in Figure 8, for both the Arecibo and Venera data sets. A sketch map showing the traces of the CSDs is displayed in Figure 8*c*. All of the CSDs are mappable for up to 1000 km across the high backscatter portion of Maxwell Montes, where they exhibit a spacing of 15-100 km. In addition, by utilizing high contrast linear stretches of digital images of this region, some of the CSDs can be observed to continue to the east-southeast for up to 100 km from the high-backscatter boundary. However, along the northern, southern, and western edges of Maxwell, the CSDs all terminate at or before the high backscatter boundary. This is not surprising since the plains

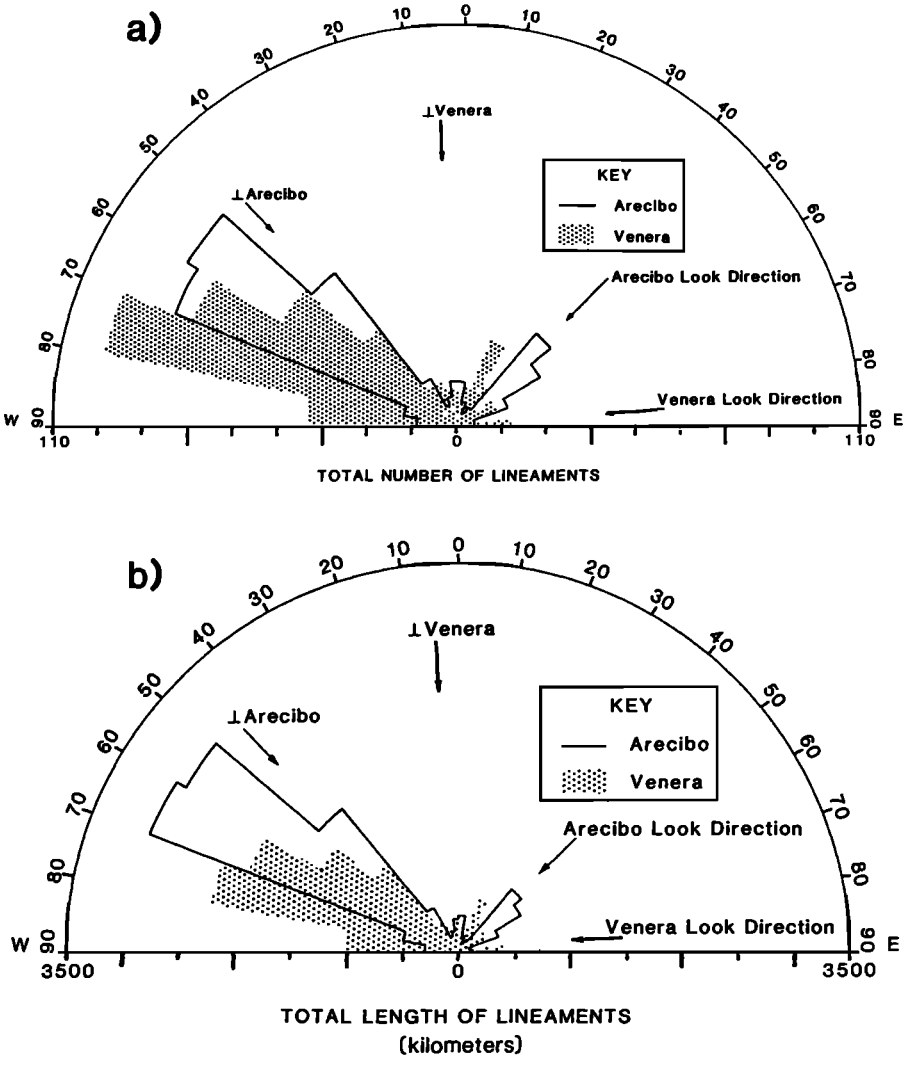

Fig. 7. Rose diagrams of Arecibo (outlined) and Venera (stippled) lineaments. Bin size is 10°. (*a*) Total number of lineaments. (*b*) Total length of lineaments.

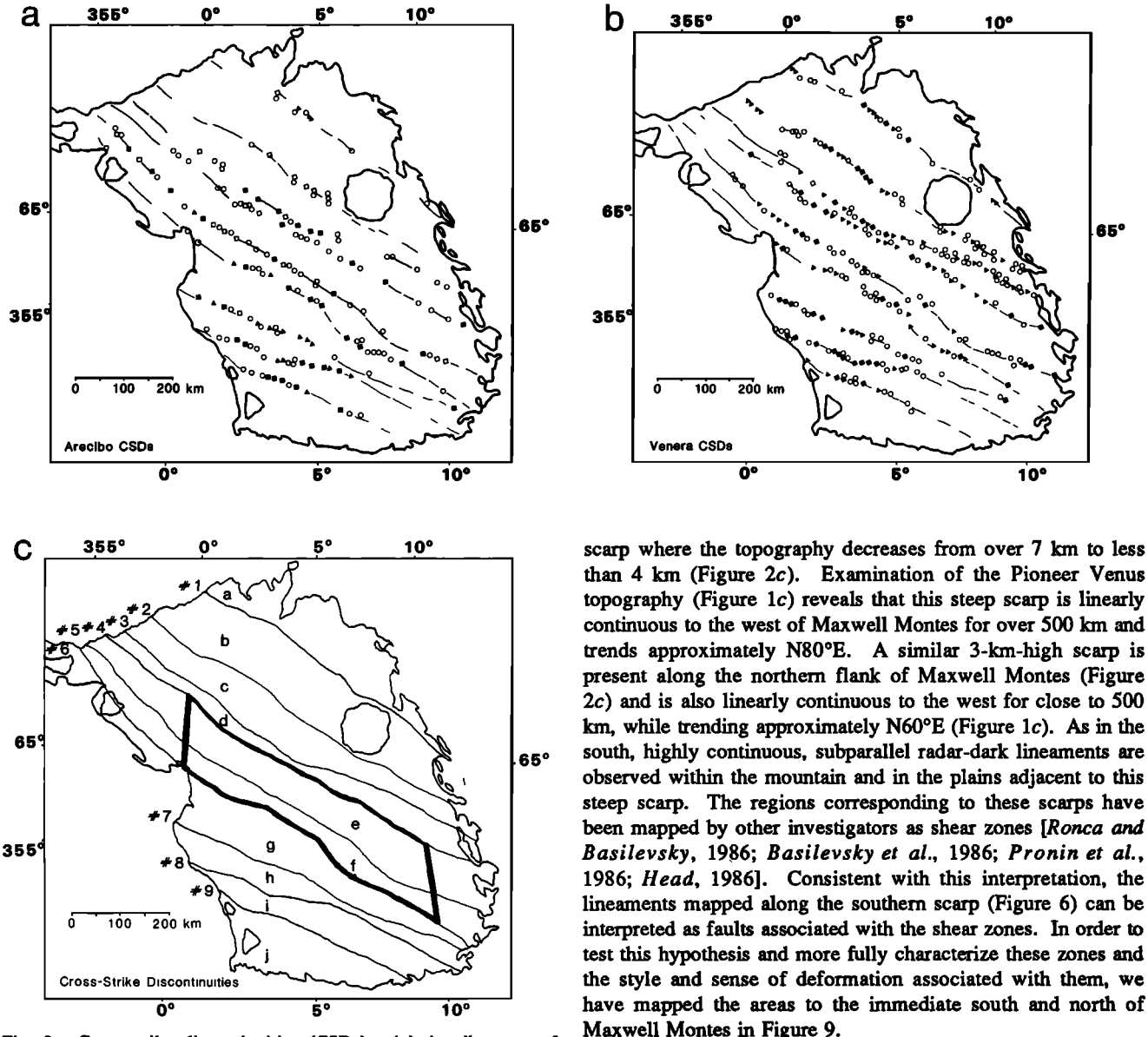

Fig. 8. Cross-strike discontinuities (CSDs). (*a*) Arecibo map of features defining CSDs. Circles represent ridge terminations, triangles represent changes in the width of ridges (>50%), open boxes represent changes in strike, solid boxes represent changes in width and strike, and heavy lines represent lineaments. (*b*) Venera map of features defining CSDs. Symbols as in Figure 8*a*. (*c*) Simple sketch map showing location of CSDs across Maxwell Montes. The CSDs are numbered 1-9 from north to south and divide Maxwell Montes into 10 crustal domains, identified here as a-j. Area in bold outline is that shown in Figure 10.

materials in these regions are relatively smooth and appear to have undergone minimal tectonic deformation in the form of the dark ridges and the extensional chasmata southwest of Maxwell. It is possible that plains materials could have buried CSDs in these regions. On Maxwell, these features have been recognized as topographic troughs in radar image stereo pairs (A. Pronin, personal communication, 1986).

Shear zones. The alignment of individual lineaments into semicontinuous linear features is also observed along the southern flank of Maxwell Montes, particularly within the Venera lineament map (Figure 6). These lineaments trend parallel to this southern flank which is characterized by a steep scarp where the topography decreases from over 7 km to less than 4 km (Figure 2*c*). Examination of the Pioneer Venus topography (Figure 1*c*) reveals that this steep scarp is linearly continuous to the west of Maxwell Montes for over 500 km and trends approximately N80°E. A similar 3-km-high scarp is present along the northern flank of Maxwell Montes (Figure 2*c*) and is also linearly continuous to the west for close to 500 km, while trending approximately N60°E (Figure 1*c*). As in the south, highly continuous, subparallel radar-dark lineaments are observed within the mountain and in the plains adjacent to this steep scarp. The regions corresponding to these scarps have been mapped by other investigators as shear zones [*Ronca and Basilevsky*, 1986; *Basilevsky et al.*, 1986; *Pronin et al.*, 1986; *Head*, 1986]. Consistent with this interpretation, the lineaments mapped along the southern scarp (Figure 6) can be interpreted as faults associated with the shear zones. In order to test this hypothesis and more fully characterize these zones and the style and sense of deformation associated with them, we have mapped the areas to the immediate south and north of Maxwell Montes in Figure 9.

The Venera image is used for this mapping since these regions are areas of relatively low radar return to the Arecibo system. The structural mapping of southern Maxwell (Figure 9*b*) shows that in addition to the north trending ridges associated with the mountain belt and the lineaments cutting across them, there are additional sigmoidal ridges striking approximately N70°W, at low angles (approximately 30°) to the trend of the lineaments. Anticlinal structures similar to these ridges are commonly observed cutting across terrestrial strike-slip faults at low angles [*Harding*, 1974, 1976], and the orientation of these features is determined by the sense of shear along the faults. The ridges associated with the N80°E trending lineaments in southern Maxwell strike N70°W, which is consistent with a left-lateral sense of shear, so that the region to the north of the shear zone (Maxwell Montes) is moving west relative to the region to the south. This sense of shear is the same found for this zone by *Ronca and Basilevsky* [1986] and *Pronin et al.* [1986]. *Ronca and Basilevsky* [1986] based their conclusion on the apparent deflection of the long, arcuate troughs in the plains southwest of Maxwell (Figures 1 and 2).

The N60°E trending shear zone to the north of Maxwell Montes is characterized by dark lineaments following the trend

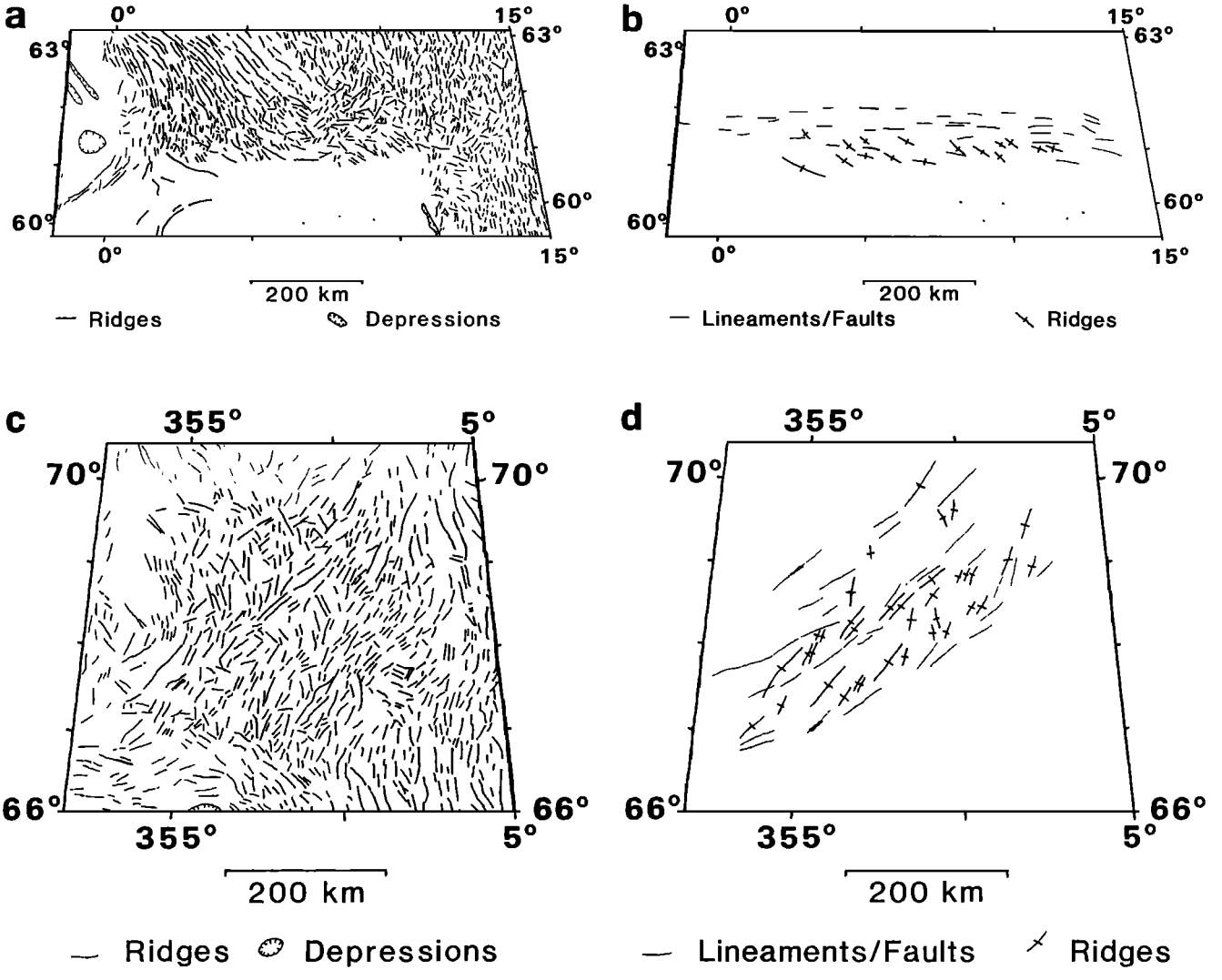

Fig. 9. Structural mapping of shear zones to the south and north of Maxwell Montes. (*a*) Structural map of southern Maxwell Montes showing all ridges (plain lines) and large, distinctive troughs (hatchured lines). (*b*) Sketch map of southern Maxwell Montes showing lineaments (plain lines) and ridges (hatched lines) used in characterizing this region as a shear zone. The lineaments are thought to represent faults, while the ridges shown are in an orientation such that they could have formed due to left-lateral shearing. (*c*) Structural map of northern Maxwell Montes showing all ridges (plain lines). (*d*) Sketch map of northern Maxwell Montes showing lineaments (plain lines) and ridges (hatched lines) used in characterizing this region as a shear zone. The ridges shown are in an orientation such that they could have formed due to right-lateral shearing.

of N60°E and large swales and individual sigmoidal ridges that strike approximately N30°E (Figure 9*d*). These ridges and swales are similar to the ridges observed in southern Maxwell (Figure 9*b*), and their orientation relative to the lineaments indicates that the shear zone has a right-lateral sense of shear. This indicates that the region south of the shear zone (i.e., Maxwell Montes) is moving west relative to the region to the north. The senses of shear along the northern and southern shear zones indicate that Maxwell Montes is moving to the west relative to the low regions flanking the mountain range to the north and south. The relative movement appears to be confined within the two shear zones because the areas north and south of Maxwell exhibit relatively little deformation in comparison to that observed on the mountain belt.

The sense of offset determined along these shear zones is consistent with the formation of Maxwell Montes through east to west crustal convergence and thickening, which we had determined earlier based solely on the topography and morphology of central Maxwell, particularly the NNE trending ridges and valleys. The movement of crustal materials from east to west and their deformation through folding, thrusting, and stacking would produce the ridges and valleys in central Maxwell, while movement along the shear zones would produce both the sigmoidal ridges and disruption in preexisting ridges observed adjacent to these zones. These observations indicate that a process of east-west compression within two converging shear zones was important in the formation of Maxwell Montes. Other processes, such as strike-slip faulting, are expected to have also played a role in the deformation of this region.

Interpretation of Maxwell Montes cross-strike discontinuities as strike-slip faults. Long, linear features are common on the surfaces of the terrestrial planets and have been attributed to a variety of origins including: planetary grids; impact basin radial structures; fracture zones analogous to those found in terrestrial ocean basins; extensional fault

troughs or graben; and strike-slip faults and shear zones. Of all these potential origins, we find that the data are most consistent with an origin as strike-slip faults on the basis of the presence of the CSDs within a compressional environment; their great length and continuity; their disruption of ridge and valley structure within the mountain range; and the correlation of individual structures across the CSDs when individual offsets are restored. These CSDs are thus different from CSDs mapped in Aphrodite Terra that are interpreted as analogs to oceanic transforms and fracture zones [*Crumpler et al.*, 1987; *Head and Crumpler*, 1987].

Cross-strike discontinuities on the Earth are recognized as strike-slip faults within at least two structural settings: (1) long, continuous linear features that occur at relatively low angles to the strike of compressional features [*Tapponnier et al.*, 1982]; and (2) shorter linear features that occur at higher angles (often normal) to the strike of compressional ridges and that may represent deformation between slightly decoupled blocks [*Wheeler*, 1980]. The former features are widely known as "wrench" or "transcurrent" faults and generally involve the basement, while the latter features have commonly been called "tear faults" and generally represent "thin-skinned" deformation [*Sylvester*, 1984]. Several observations (including the low angle at which the CSDs occur relative to the compressional ridges and troughs, their length and continuity, and the fact that ridges are seen to terminate or change character at them) have led us to investigate the hypothesis that the CSDs represent large-scale, "wrench"-type, strike-slip faults.

Nature of potential offset along CSDs and retrodeformation. The nine cross-strike discontinuities divide Maxwell Montes into 10 crustal domains. We have examined neighboring domains and attempted to determine any relative motions between them by matching major topographic features (such as ridges) across the CSDs. An illustration of this technique is shown in Figure 10. In Figure 10*a*, portions of domains e and f (to the north and south of CSD 5, Figure 8*c*) are shown as seen in the Arecibo data. A sketch map of the observed configuration, showing major ridge segments is shown in Figure 10*b*. Segments labelled I to III either terminate against or exhibit a change in character at the CSD. By matching these major ridge segments across CSD 5, a best visual fit was achieved as shown in Figure 10*c*. A sketch map of this reconstructed configuration is shown in Figure 10*d*. The reconstruction suggests that features I, II, and III were once longer, continuous features that have been disrupted by strike-slip faulting along CSD 5 and offset relative to one another. We interpret the reconstruction to indicate that a right-lateral offset of 125 km has occurred along CSD 5. Similar reconstructions made between neighboring domains indicate that right-lateral offsets ranging from 10 to 125 km have occurred along each CSD. The offsets along each CSD were determined in the same manner as for CSD 5, and are given in Table 3.

The right-lateral sense of offset determined in our reconstructions is an unexpected result. The ridges on Maxwell Montes strike approximately N20°W-N40°W, indicating a greatest principal stress axis perpendicular to them at N70°E. If strike-slip faults formed in this environment, they would be expected to have a strike of approximately N80°W or N40°E (30° from the greatest principal stress direction, assuming that the fault strength is approximately equal to the average strength of terrestrial crustal material). This is quite different from the N55°W orientation of the observed cross-strike discontinuities. In addition, although high-angle strike-slip faulting is not impossible in a compressional environment, the right-lateral offsets observed along the CSDs in Maxwell Montes are in the opposite direction from what would be predicted in the stress field that produced the ridges. Instead, the CSDs and their right-lateral offsets are more consistent with a greatest principal stress axis which trends approximately N25°W, which is almost parallel to the strike of the ridges.

Following the identification of matching features, relative directions of offsets, and absolute offsets for adjacent domains, it is then possible to generate a reconstruction of all 10 domains of the mountain range (Figure 11*a*). The individual features which were used to determine offsets between adjacent domains are, of course, now continuous across the CSDs. A number of additional major features not used in the matching of offsets (labeled A-D in Figure 11*b*) appear to correlate across the CSDs in the reconstructed Maxwell Montes. Feature A is a 30-km-wide, bright/rough lineament that crosses four CSDs and is continuous for over 200 km. Feature B is a single, distinctive ridge running for over 400 km and across four CSDs, and feature C is a pair of parallel ridges extending for over 700 km and across five CSDs. Finally, feature D represents a 400-km-long, continuous boundary between the bright/rough, dissected terrain unit in the east and the banded units to the west. These correlations suggest that the reconstruction of individual offsets in each CSD has produced a configuration which reveals additional throughgoing structure that existed prior to the formation of the cross-strike discontinuities.

In order to assess more thoroughly the validity of this reconstruction, the process was repeated using the Venera data (Figure 11*c*), the topographic map (Figure 11*d*), and the geologic map (Figure 11*e*), but assuming the same offsets recognized in the Arecibo data (Figure 11*a* and Table 3). Comparison of the reconstructions based on each data set reveals a close correspondence. Just as the Arecibo reconstruction shows the 400-km-long, continuous boundary between the rough, complex dissected terrain in the east and the banded units to the west, so does the Venera reconstruction. In addition, the Venera reconstruction reveals a single, contiguous unit of smooth deposits associated with Cleopatra (Figure 11*c*). In contrast, in the geologic map of present-day Maxwell Montes (Figure 2*d*) the smooth deposits are distributed in two separate locations, with the majority around Cleopatra and an outlier to the southwest in central Maxwell. Cleopatra and the smooth deposits are found between two regions of dissected terrain which the smooth deposits appear to embay. The relationship between the dissected terrain unit and the bright terrain deposits in the reconstructed unit map suggests that a relative age relationship can be established for these units and the strike-slip faulting along the CSDs. The continuity of these units and their boundaries in the reconstruction but not in the present configuration suggests that they formed uninterruptedly before strike-slip faulting disrupted them and produced the observed offsets. In addition, the apparent embayment of the dissected terrain by the bright terrain indicates that the dissected terrain formed before the bright terrain. These relationships suggest that the ridges and valleys of the banded units and dissected terrain formed first, followed by emplacement of the bright terrain embaying and disrupting the continuity of the dissected terrain, after which CSD formation occurred, accompanied by strike-slip faulting, culminating in the mountain range observed today.

Although the majority of ridges are continuous across the

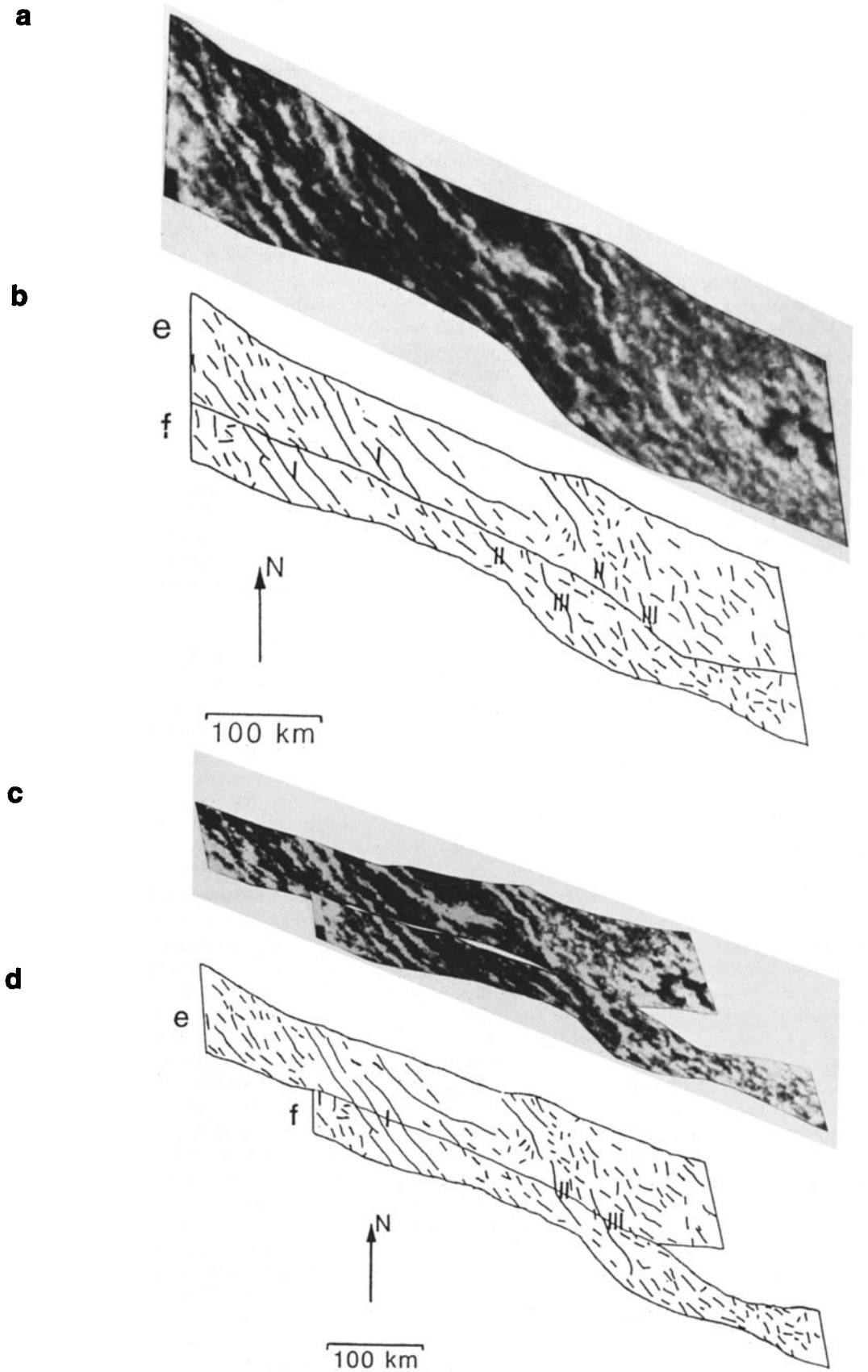

Fig. 10. Identification of cross-strike discontinuities as strike-slip faults and determination of the amount and sense of offset along them. (*a*) Location shown in Figure 8*c*. (*a*) Arecibo image and (*b*) sketch map of portions of domains e and f shown in Figure 3*a*. CSD is long, solid, east-west line that separates the two domains, ridges are the less continuous solid lines. Note the sets of three ridges marked I, and the individual ridges marked II and III. (*c*) Image and (*d*) sketch map of "best fit" of domains e and f. This shows continuous features I, II, and III. This technique indicates an offset of 125 km in a right-lateral sense.

TABLE 3. CSD Offsets (All Right-Lateral)

CSD	Offset, km
1	40
2	30
3	120
4	20
5	125
6	35
7	80
8	25
9	80

CSDs, some ridges have no corresponding ridge across the CSD at which it terminates. The simplest explanation is that these ridges were never disrupted by a CSD. Instead, they initially formed as ridges which terminated where the CSD later cut through. Therefore such a ridge would not be expected to have a corresponding ridge across a CSD. A second possibility is that a few of these ridges represent features that formed during strike-slip deformation. En echelon folds and pull-apart graben are often associated with terrestrial strike-slip environments, such as along the San Andreas fault zone [*Crowell and Ramirez*, 1979]. These features form as a result of compression or extension localized near a strike-slip fault during motion along the fault. Such features are not always continuous across the fault but may form individually on one side or the other. This fact, combined with the possibility that these features can form at any stage of strike-slip motion, means that there may be some ridges or troughs that terminate against a CSD in the reconstruction, with no continuation across the CSD.

In contrast, *Garfunkel and Ron* [1985] describe a similar type of deformation during large-scale block rotation along subparallel strike-slip faults. Their work indicates that the interior of adjacent, rotating crustal blocks may remain largely undeformed, while the boundaries of these blocks accommodate the majority of the strain and deform in order to maintain mutual contact between blocks. Similarly, we conclude that the major features used to determine the sense and amount of offset between the crustal domains of Maxwell Montes could remain largely undeformed during offset and that minor features which terminate at CSDs do not contradict the large-scale reconstruction and strike-slip offsets of up to 125 km.

Returning to the large scale, a further assessment of the model of retrodeformation can be made by examining the topography of Maxwell Montes. The present topography of Maxwell Montes is illustrated in Figure 2*c*. We have retrodeformed the present topography to a pre-strike-slip form (Figure 11*d*) as we did with the Venera image, using the offsets determined from the Arecibo image reconstruction. Since strike-slip faulting occurs for the most part in the horizontal plane, we consider it reasonable to reconstruct topography along strike-slip faults. However, we note that smaller-scale topographic features might be produced or destroyed during strike-slip motion, just as we described the possible production of en echelon folds or pull-apart graben above. With this caveat in mind, we note that this reconstruction brings the initially hummocky crest and the steep western slope of the mountain into a linear configuration and maintains the parallelism of contours on the western slope and the asymmetric profile with a steep western slope and more gentle eastern slope.

Initial configuration of proto-Maxwell Montes. The initial topographic configuration of the retrodeformed proto-Maxwell Montes (Figure 11*d*) is similar to that of the Akna Montes linear mountain belt in western Ishtar Terra (Figure 12). In particular, although the relief of Maxwell Montes is nearly twice that of Akna, both proto-Maxwell Montes and Akna Montes exhibit a general topographic pattern with an asymmetric profile and a long linear crest running parallel to the strike of the mountain (Figures 11*d* and 12*c*).

The reconstructed image mosaics (Figures 11*a* and 11*c*) depict a mountain range with a smooth pattern of long, linear ridges, similar to that of the 1000-km-long Akna Montes (Figures 12*a* and 12*b*). These long, linear ridges occur along the steep western slope and summit portions of proto-Maxwell Montes (Figures 11*a* and 11*c*), while shorter, discontinuous ridges and dissected terrain occur along the more gentle eastern slope. In Akna Montes, long, linear ridges occur along the steep eastern slope and summit portions, while shorter, discontinuous ridges and dissected terrain are found on the gentle western slope (Figures 12*a* and 12*b*). The similarity of these patterns is reflected in a comparison of the unit maps of proto-Maxwell Montes (Figure 11*e*) and Akna Montes (Figure 12*d*), as well as with Freyja Montes [*Head*, 1990]. Finally, "proto-Maxwell Montes" is 300 km in width and 1200 km in length, is slightly larger than Akna Montes (250 km by 1000 km), but has the same aspect ratio.

TECTONIC SYNTHESIS

The similarities between proto-Maxwell Montes and Akna Montes lead us to hypothesize that Akna may represent the initial, relatively simple form of compressional orogenic belts on Venus and that the deformation which produced the present Maxwell Montes occurred in at least two stages. In the first stage, proto-Maxwell Montes formed as an Akna-like linear mountain belt through compressional deformation, with the greatest principal stress oriented perpendicular to the strike of the ridges. This initial linear mountain belt had a steep western slope which may have represented the deformational front and a linear crest. This initial mountain belt had long continuous ridges on its western and central, summit regions, with less continuous ridges in the form of dissected terrain to the east. Then, sometime after the formation of the Cleopatra circular feature and its associated deposits, a reorientation of the principal axes of stress resulted in right-lateral strike-slip offsets of up to 125 km across the cross-strike discontinuities, producing the presently observed mountain range. The initiation of strike-slip faulting in the second stage of deformation need not be accompanied by a termination of first stage-type compressional deformation. During large-scale strike-slip offset, additional folding and mountain building could continue due to the original compressional forces, but they would not produce features continuous across the CSDs. Therefore the description of multiple stages in the evolution of Maxwell Montes indicates a distinction in the styles of deformation, not necessarily an unambiguous sequence involving the termination of one process followed by the initiation of another. We now proceed to describe and assess several models for the multistage deformation.

Three models for the evolution of Maxwell Montes are presented in Figure 13. The models all reflect the initiation of Maxwell Montes as an Akna Montes-like linear mountain belt followed by large-scale strike-slip faulting to generate the observed configuration. The three models differ in the processes through which strike-slip faulting is initiated and

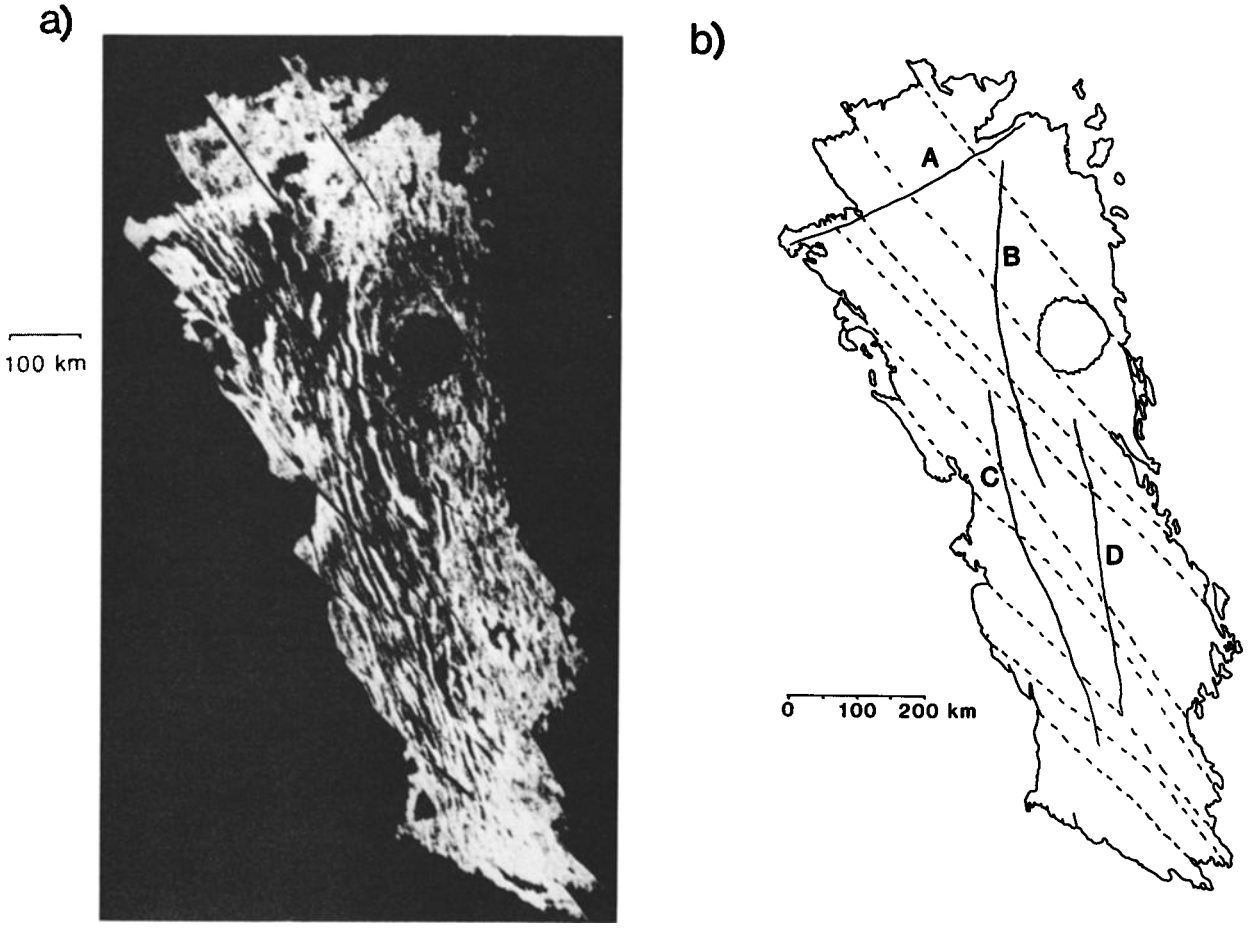

Fig. 11. Retrodeformation of Maxwell Montes: (*a*) Arecibo image reconstruction generated through technique shown in Figure 10. All succeeding reconstructions use offsets determined from this technique. (*b*) Sketch map of reconstructed Arecibo image, showing long, continuous, linear features. A, a 30 km-wide bright lineament continuous for over 200 km that crosses four CSDs. B, a 15 km-wide ridge continuous for over 400 km across four CSDs. C, two parallel ridges continuous for over 700 km across 5 CSDs. D, a 400 km-long linear boundary between the dissected terrain unit to the east and the banded units to the west. (*c*) Venera image reconstruction. (*d*) Topographic reconstruction. Contour interval is 1 km, with values relative to mean planetary radius of 6051.0. Note the linearity of the crest in this reconstruction relative to the hummocky nature in Figure 2*c*. (*e*) Reconstructed geological unit map. Note continuity of dissected terrain and bright terrain units.

accomodated. The first two models (Figures 13*a* and 13*b*) suggest that proto-Maxwell formed in its present location and then underwent strike-slip deformation either with or without large-scale rotation of the entire mountain belt. The third model (Figure 13*c*) suggests that the strike-slip faulting was related to large-scale east-west migration of the range within two converging shear zones, either with or without rotation.

In-place formation, without rotation. In the first model (Figure 13*a*), proto-Maxwell Montes has formed as an Akna Montes-like linear mountain belt striking north-northwest. This is then followed by a reorientation of the greatest compressional stress to N25°W in order to generate the observed orientation of CSDs and the offset along them. This model assumes that the orientation of the CSDs has remained fixed at N55°W during the strike-slip faulting. If Maxwell remained centered at 5°E/65°N with little or no large-scale rotation during offset (Figure 13*a*), then there should be evidence for N25°W directed compression to the north and south, perhaps in the form of folding or thrusting. As described above, the northern and southern slopes of Maxwell are characterized by the transitional units which are dominated by NNW trending ridges and valleys that often terminate against ridge-perpendicular troughs and by steep slopes associated with the shear zones. Although none of these features are strongly indicative of NNW-SSE compression, the steep scarps that extend west-southwest from northern and southern Maxwell are flanked by broad linear rises up to 100 km across on the edge of Lakshmi Planum (Figure 1). This combination of a broad topographic rise and an adjacent steep scarp is similar to that of Danu Montes along the southern flank of Lakshmi Planum which has previously been interpreted as the result of compressional deformation [*Pronin et al.*, 1986; *Head*, 1986]. Although the surface morphology of these rises does not include WSW oriented subparallel ridges and valleys as in Danu, these rises could be related to some NNW-SSE convergence. Several workers have recently discussed styles and orientations of crustal convergence around Ishtar Terra [*Head*, 1990; *Vorder Bruegge and Head*, 1989*a*; *Kozak and Schaber*, 1989]. *Head* [1990] describes the formation of Freyja Montes and the adjacent region, Itzpapalotl Tessera, as due to north-south convergence and underthrusting of the North Polar Plains beneath Ishtar Terra.

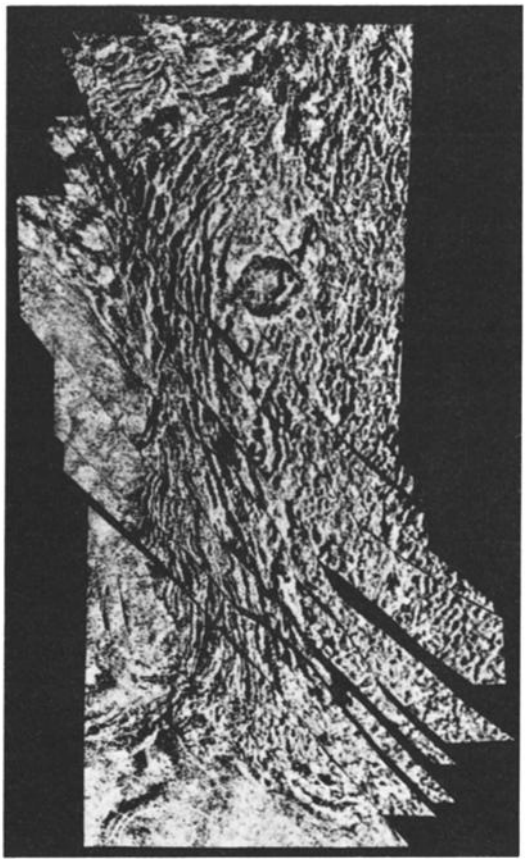

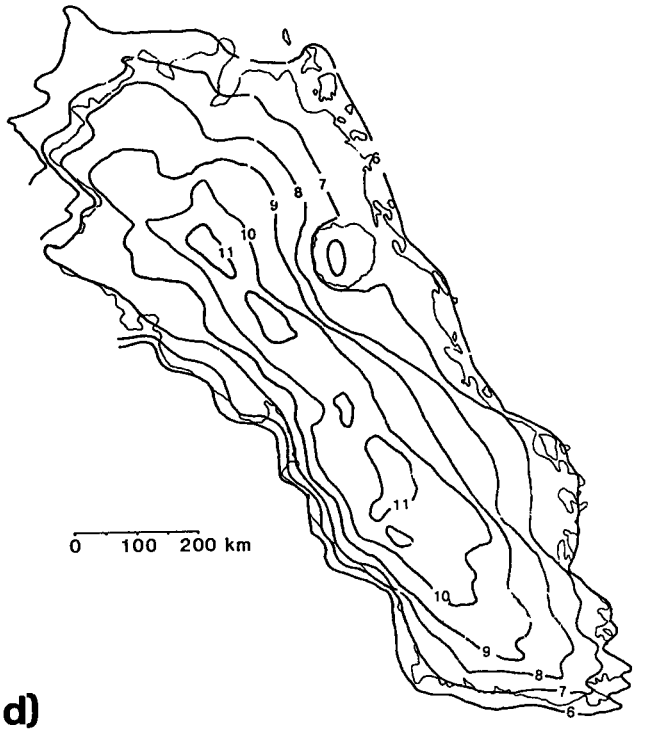

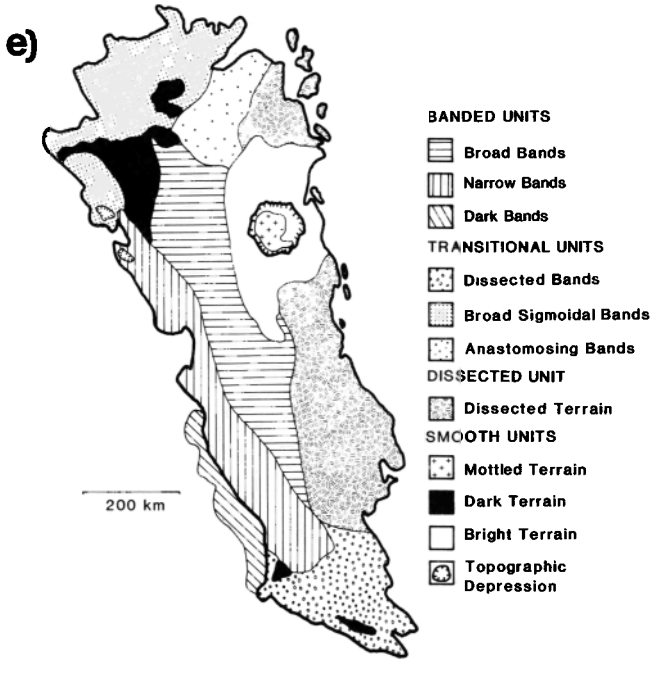

Fig. 11. (continued)

Vorder Bruegge and Head [1989*a*] have shown that similar underthrusting oriented NNE-SSW occurs elsewhere along the northern boundary of Ishtar Terra. In contrast, *Kozak and Schaber* [1989] suggest that WNW directed crustal spreading is occurring approximately 1000 km to the southeast of Maxwell. Thus, although a simple model of NNW-SSE directed convergence may be suggested by the broad linear rises to the west of Maxwell Montes, such a model is not supported by the small scale surface morpholgy which lacks ridges and valleys nor by the regional observations which suggest different directions of crustal convergence in this region. However, it is uncertain if the necessary reorientation of stresses could be accomplished through a combination of different convergence events and/or orientations.

In-place formation, with rotation. In the second model (Figure 13*b*), after formation of the Akna-like proto-Maxwell Montes, a reorientation of stresses results in the formation of the CSDs and strike-slip offset along them, accompanied by large-scale rotation of the mountain belt, which remains centered at 5°E/65°N. This differs from the first model in that the orientation of the CSDs changes during strike-slip faulting. Using the simple block rotation model of *Garfunkel and Ron* [1985], the right-lateral offsets of the Maxwell Montes domains would result in right-lateral shear along the entire boundary and a counterclockwise rotation of the domains (and the CSDs) relative to the boundary. If such an overall counterclockwise rotation of the mountain belt occurred, then the general strike of proto-Maxwell Montes would have been closer to north-south than is presently observed (Figure 13*b*). Although it is uncertain how much overall rotation could have taken place, if proto-Maxwell was oriented in a north-south configuration, then the north-south directed convergence interpreted to occur along northern Ishtar Terra [*Head*, 1990; *Vorder Bruegge and Head*, 1989*a*] is in the correct orientation to produce the strike-slip faulting and offset observed in Maxwell Montes. However, an observation that contradicts this model is that the sense of shear along the boundary of

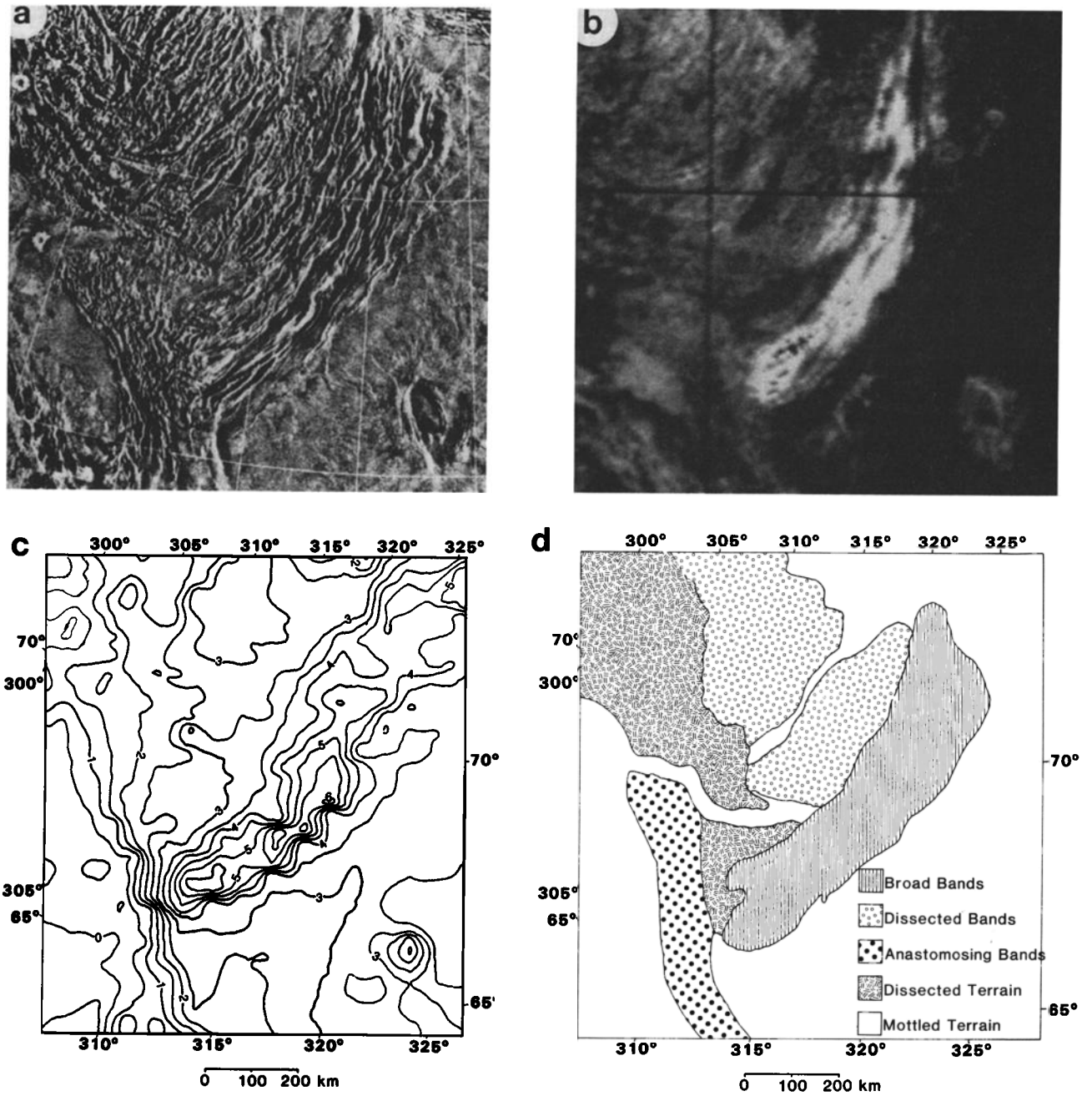

Fig. 12. Akna Montes. (*a*) Venera and (*b*) Arecibo images. (*c*) Topography of Akna Montes (Venera topography). (*d*) Geological map comparable to Maxwell Montes unit map (Figure 2*d*).

Maxwell Montes is not consistently right-lateral. Although there is a right-lateral sense of shear along the northern boundary of Maxwell, the southern boundary displays evidence of left-lateral shear (Figure 9), and the eastern and western boundaries of the range show no evidence for large-scale shear at all. These observations indicate that strike-slip faulting associated with simple rotation of Maxwell Montes as a whole cannot account for all of the features observed in and around the mountain belt. Indeed, we have already seen that the plains regions west of Maxwell show evidence of tectonic and volcanic activity different from that observed on the mountain range. In particular we note the interpreted formation of the dark bands from plains materials and a lack of CSDs within this unit and within the plains units beyond. These observations suggest that tectonic deformation continued in this region after activity along the CSDs ceased. Additionally, the east-west convergence of materials from Fortuna Tessera to Maxwell [*Vorder Bruegge and Head*, 1989*b*] could produce overprinting of patterns in eastern Maxwell and may be responsible for the observed sense of shear along southern Maxwell. High-resolution images obtained by the Magellan spacecraft should clarify this sequence of events and help determine if this model and further deformation could account for all of the deformation observed here.

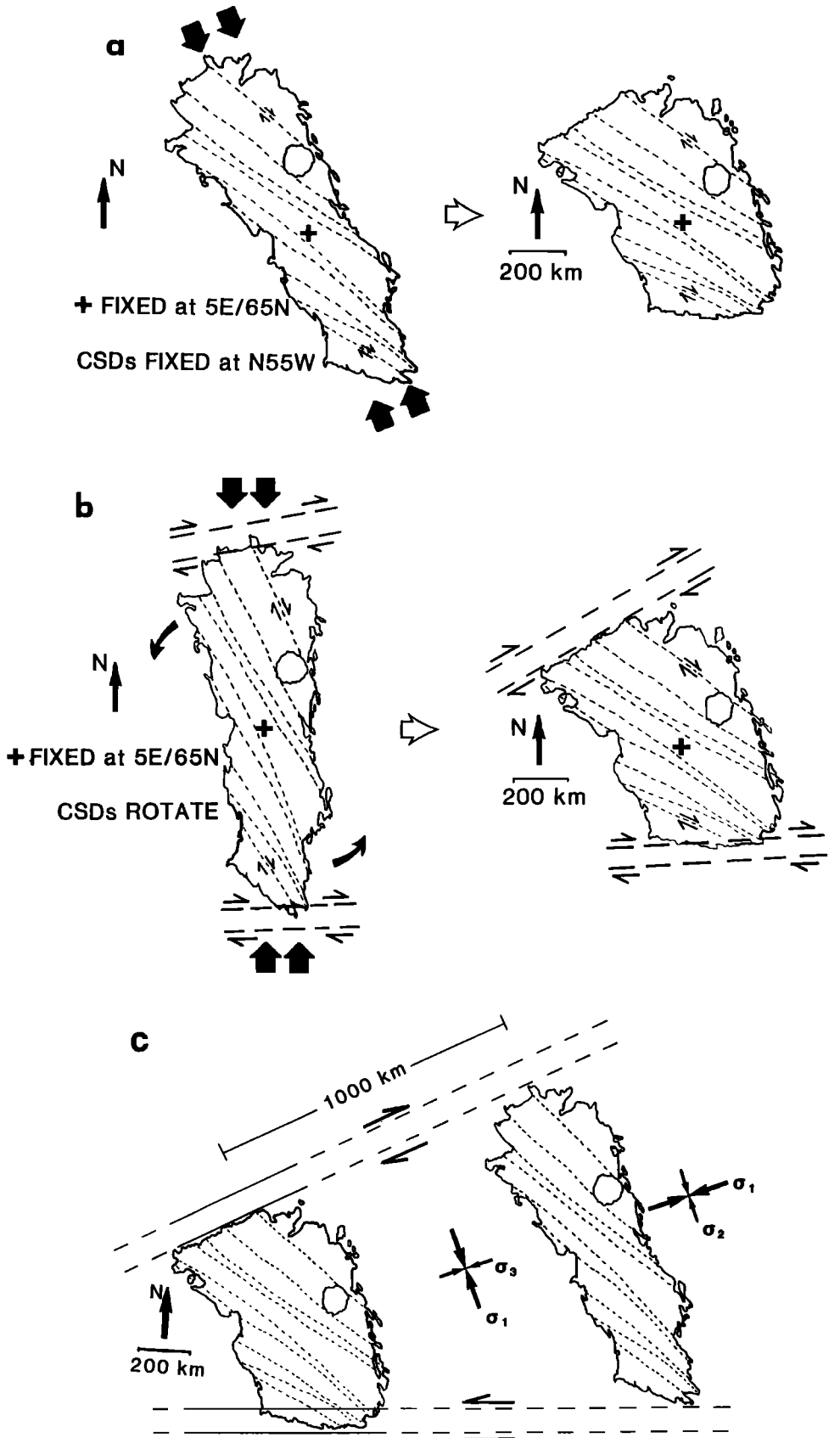

Fig. 13. Models of strike-slip deformation of Maxwell Montes, following creation of proto-Maxwell Montes. (*a*) In-place, strike-slip offset with no rotation of the CSDs. Domain e remains stationary while the other domains move relative to it. This requires NNW-SSE compression as indicated by the large arrows. (*b*) In-place, strike-slip offset with rotation of the CSDs. The point marked by the cross at 5°E/64°N is considered fixed, while the domains are offset. The domains and CSDs are then effectively rotated. (*c*) Lateral movement of Maxwell Montes within two converging shear zones. Overall rotation may or may not occur in addition to east-west motion, so the maximum possible offset, defined by the geometry of the shear zones, the reconstruction, and the assumption of no rotation is shown. A lateral transport of Maxwell Montes to the west over 1000 km is indicated by this geometry.

Lateral migration within two converging shear zones. We also consider the evolution of Maxwell Montes during strike-slip faulting without large-scale rotation but accompanied by shear along the northern and southern boundaries (Figure 13*c*), as suggested by the different senses of shear observed along the northern and southern zones of Maxwell. The right-lateral sense of shear along the northern shear zone and the left-lateral sense of shear along the southern shear zone suggest that we should consider a model in which the shear zones are essentially fixed in space and deformation occurs within a wedge-shaped zone whose apex is to the west and which opens to the east. If the direction of deformation is along a bisector of the angle of the wedge, then strike-slip deformation along faults oriented in the same direction as the CSDs would be right-lateral, and features and structures would be faulted and shortened without significant rotation. The evolution of crustal materials moving within two converging fracture zones has been discussed for the Gorda plate on Earth [*Bolt et al.*, 1968; *Wilson*, 1986; *Stoddard*, 1987]. The lateral movement of materials between converging fracture zones acts to produce compressional stresses perpendicular to the direction of motion, across the fracture zones. *Wilson* [1986] and *Stoddard* [1987] both suggest that these stresses could produce strain in the crust across the fracture zones; one way to accommodate this strain would be by strike-slip faulting which shortens crustal material in a direction perpendicular to the fracture zones. This configuration and geometry are consistent with the features and sense of offset in Maxwell Montes. We suggest that a similar mechanism may have been involved for the Maxwell Montes shear zones. As in the terrestrial model, we envision the areas outside the shear zones as "stable" crustal blocks, between which crustal materials were transported laterally. During this phase, the greatest principal stress axis would be oriented perpendicular to the strike of the ridges and the minimum principal stress axis would be vertical. In order for strike-slip faulting to occur as observed, the greatest principal stress must have been parallel to the strike of the ridges, and the minimum principal stress must have been perpendicular to the ridges in the horizontal plane, while the intermediate principal stress axis was vertical. As the orogeny continued and proto-Maxwell Montes grew within the converging shear zones, the topography would have increased to produce a greater vertical load. We suggest that strike-slip faulting occurred once proto-Maxwell Montes had thickened enough to produce a nonhydrostatic vertical load in excess of whatever residual E-W compression existed.

The strike-slip movement of the crustal domains in Maxwell Montes is identical to that discussed for rotating crustal blocks by *Garfunkel and Ron* [1985], except that the primary rotation has been inhibited by the shear zones to the north and south. The deformation is accommodated by a combination of large-scale offset and small-scale internal deformation along the strike-slip faults and shear deformation along the northern and southern boundaries of Maxwell Montes. The lack of large-scale deformation within the crustal domains suggests that the upper portions of these blocks were relatively strong during the strike-slip offset and that this offset accommodated the majority of the strain. It is expected that such offset would be acompanied by more evenly distributed deformation at depth, where the rocks there are more ductile, as *Garfunkel and Ron* [1985] suggest for Earth.

A recent study [*Vorder Bruegge and Head*, 1989*b*] supports the interpretation that east-west convergence is the dominant process affecting Maxwell Montes and the area to the east. Westernmost Fortuna Tessera exhibits evidence of large-scale compressional deformation and crustal thickening in the form of high topography and north trending ridges and valleys for hundreds of kilometers to the east of Maxwell Montes. These observations indicate that east-west convergence is not restricted to Maxwell Montes.

Using the geometry of the converging shear zones, the configurations of Maxwell Montes and proto-Maxwell Montes, and assuming no rotation of the domains relative to the shear zones, it is possible to estimate the maximum westward distance travelled by the domains within the shear zones (Figure 13*c*). On the basis of this reconstruction (Figure 13*c*) we suggest that Maxwell Montes could have originally occupied a position as much as 1000 km to the east. We interpret the observed features and structures to suggest that during the transport of Maxwell Montes to the west it was wedged between the two converging shear zones, causing the reorientation of the maximum principal stress to a more north-south configuration. The mapped shear zones strike N60°E and N80°E, suggesting lateral movement within the shear zones along a trend of approximately N70°E, approximately the same trend necessary to produce compressional ridges on Maxwell Montes that strike N20°W-N40°W. This suggestion is consistent with no rotation of the domains during westward transport since the presently observed ridges on Maxwell Montes strike approximately N20°W-N40°W, as would the ridges on proto-Maxwell Montes. In addition, if compression then occurred perpendicular to these shear zones, then the axis of compressional stress would shift to N20°W, indistinguishable from the N25°W trend inferred from the strike of the cross-strike discontinuities.

As in the other models, this lateral transport and strike-slip faulting would have produced the offset of large-scale linear and curvilinear features such as ridges, valleys, unit boundaries, and topographic contours (Figure 11). In addition, other features off the mountain range could have been produced during this large-scale lateral transport. One such example is the addition of relief along the shear zones, due to the convergence of the crustal blocks undergoing strike-slip movement. *Stoddard* [1987] showed that the convergence of crustal materials within two oblique shear zones results in the "piling up" of material along the fracture zones. For example, a linear topographic high resulting from such a process is observed along the Mendecino Fracture Zone on Earth [*Stoddard*, 1987]. A similar increase in topography is observed along the two shear zones for distances of up to 500 km to the west of Maxwell Montes (Figure 1*c*); these are the linear "rises" which could alternately be linked to the NNW-SSE convergence suggested in the model of Figure 13*a*.

The coincidence of the strike of the ridges and the trends of the shear zones may favor the hypothesis that these features are intimately linked by a single continuous process of ENE-WSW crustal convergence within the shear zones. The shear zones would thus represent a genetic link between the present Maxwell Montes (Figure 2) and the Akna-like proto-Maxwell Montes (Figure 11). From the geometry of the shear zones and the present and reconstructed Maxwell Montes and assuming no rotation of the CSDs, it is possible to place proto-Maxwell Montes within the shear zones at the location where strike-slip faulting would have commenced (Figure 13*c*). With no rotation assumed during transport, the strike of the ridges remains perpendicular to the transport direction and compression. The 30% shortening of the length of Maxwell Montes, from 1200 to 800 km, is equivalent to 1000 km of horizontal offset

within the 20° opening of the shear zones (Figure 13*c*). It is important to recognize that 1000 km is a maximum value for the east-west motion of Maxwell that depends upon the assumption of equivalent offset along the north and south bounding shear zones. It is possible that some large-scale rotation could occur in addition to east-west convergence within the bounding shear zones. Such east-west movement, accompanied by large-scale rotation, could account for the observed sense of shear north and south of Maxwell, without requiring 1000 km of convergence. It is not presently possible to determine how much offset has occurred along the northern and southern shear zones, so our maximum estimate of up to 1000 km is based solely on the geometry of proto-Maxwell Montes.

If Maxwell Montes migrated to the west within the shear zones, the material in front of the advancing mountain range could have undergone several different processes or combinations of processes. First, it could have been compressed and folded into additional anticlines and synclines at the front edge of proto-Maxwell Montes. Second, it may have been pushed ahead of proto-Maxwell Montes as a single, undeformed block within the converging shear zones. Finally, the material in front could have been removed through some mechanism similar to underthrusting and/or subduction.

The creation of additional anticlines and synclines ahead of the advancing proto-Maxwell Montes would remove material from in front of Maxwell through crustal thickening and, in effect, create an additional mountain range ahead of proto-Maxwell Montes. Examination of the region far to the west of Maxwell Montes within the shear zones, in central Lakshmi Planum, does not reveal any clear evidence of a subduction zone or a mountain range there (Figure 1). This indicates that crustal materials are not being extensively removed far ahead of Maxwell Montes in Lakshmi Planum. Instead, the removal of material might be concentrated at the edge of, and/or below, the Maxwell Montes mountain range.

A mechanism similar to terrestrial subduction may be able to account for the removal of crustal material ahead of Maxwell Montes. The western slope of Maxwell is the steepest slope on the planet and exhibits regional slope and elevation characteristics similar to active continental margins and zones of continental convergence on Earth [*Sharpton and Head*, 1986]. The removal of surface materials to depth beneath Maxwell Montes could produce an increase in relief from the proto-Maxwell Montes stage to the present. However, the topographic reconstruction (Figure 11*d*) suggests that the strike-slip deformation produced no change in the topography of the mountain belt. This indicates that there could only be limited lateral migration and crutal thickening within the converging shear zones. We suggest that a combination of large-scale rotation (Figure 13*b*) and a limited lateral migration/crustal thickening of Maxwell Montes within the shear zones (Figure 13*c*) could account for the observed morphology, topography, and sense of shear.

Alternatively, we note that the topographic reconstruction (Figure 11*d*), with its steep, continuous western slope and linear crest configuration, indicates that there was no change in the relative relief of the mountain range. In generating this reconstruction, the assumption was made that only strike-slip faulting was affecting the mountain range as a whole. Although we cannot rule out the possibility that some topographic variations occurred during strike-slip deformation, there is no clear evidence to suggest the location or magnitude of these variations. Therefore we can consider only the simplest case. In such a case, it is expected that the actual relief of the mountain range would remain mostly unchanged, and from this we would infer that the initial elevation of proto-Maxwell Montes was up to 11 km. However, the model shown in Figure 13*c* suggests that in addition to large-scale strike-slip faulting, the mountain range was also undergoing some lateral movement within the converging shear zones. If up to 1000 km of lateral transport occurred during movement within the shear zones, then some change in topography would seem likely, as such extensive crustal movement is likely to have been accompanied by thickening in order to conserve crustal mass. In order to preserve the integrity of the topographic reconstruction during this lateral migration and crustal thickening, then the thickening process must have been very homogeneous. If the crustal thickening took place at depth, then we would expect it to be relatively homogenous due to the increased ductility of the rocks. Such homogeneous deformation might be capable of producing constant uplift across the entire mountain range, thus preserving the integrity of the topographic reconstruction. This uniform uplift would be analogous to a model suggested by *Zhao and Morgan* [1985] for the uniform uplift of the Tibetan Plateau.

As described by *Zhao and Morgan* [1985], a very weak layer (a fluid with a viscosity of 10 Pa s or less) is contained at depth by surrounding crustal blocks. As material is added ("injected") to this layer during lateral migration, the hydraulic pressure increases, producing a constant uplift above this layer. If the materials above this fluid layer are strong, then the relative relief should be preserved within the mountain belt, as the strong layers will not deform extensively due to uplift. Instead, the mountain belt will rise as a block. The linearity of ridges in present-day Maxwell Montes (Figure 2) and in the reconstruction (Figure 11) indicates that the ridge-parallel compressional stress, which produced the CSDs and strike-slip faulting, did not extensively deform the ridges. Some lineaments are present within individual domains (Figure 6) and may represent minor offsets of individual ridges, but unlike the CSDs, they are not linearly continuous throughout entire domains and do not appear to represent widespread penetrative horizontal shortening. Instead, the CSDs and strike-slip faulting appear to have accommodated the majority of the strain, while the individual domains between CSDs remained strong and, for the most part, internally undeformed. Therefore the upper crust in the Maxwell Montes region could be considered relatively strong and the topography could be preserved in the reconstruction.

The relatively gentle slope in eastern Maxwell Montes, in the dissected terrain, might be explained using a similar model suggested for Tibet by *Molnar and Tapponier* [1978]. While maintaining the idea of a ductile layer at depth with a constant fluid pressure, they emphasize the presence of a weak crust above it. As material is added at depth and the elevation increases with hydraulic pressure, the weak crust deforms to maintain a uniform elevation, hence the constant, gentle slope of eastern Maxwell Montes in the dissected terrain. The change in crustal strength that we suggest across Maxwell is consistent with the morphology observed across the mountain range. While the continuous ridges of the banded units may represent a strong deformational front, the disrupted ridges of the dissected terrain suggest a weak crustal layer in the hinterland.

In summary, by analogy to Akna Montes, we expect that proto-Maxwell Montes would have had a comparable topographic signature of at least 6 km. Additionally, the

topographic reconstruction (Figure 11*d*) suggests that Maxwell Montes did not experience any large-scale changes in relative relief during strike-slip faulting. However, if the movement of Maxwell within the converging shear zones was up to 1000 km, then significant amounts of crust must be removed beneath Maxwell. Mechanisms of ductile crustal thickening at depth may be capable of preserving the topographic signature of proto-Maxwell Montes during this second stage of deformation. It is therefore suggested that some large-scale uplift may have accompanied the movement of Maxwell Montes within the bounding shear zones. The importance of this mechanism of crustal uplift depends on the relative amounts of lateral transport and large-scale rotation of the mountain range during the strike-slip phase of deformation. With the present data it is unclear how these two processes are related. If Maxwell underwent more rotation, then less lateral transport is required. This, in turn, requires less material to be removed at depth, as well as less concomitant uplift, and implies that proto-Maxwell Montes originated as an 11-km-high mountain range that was oriented along a more north-south trend. High-resolution images and gravity data obtained by the Magellan spacecraft should help clarify the mechanisms of crustal compensation and the relative importance of large-scale lateral movement and large-scale crustal block rotation in the Maxwell Montes area.

Interpretation of Geological History

The evolution of Maxwell Montes interpreted from this analysis may be described as a two-stage process. In the first stage, a linear mountain belt formed through processes of compression and crustal convergence. Ridges, valleys, and high topography resulted from processes of crustal thickening including folding, thrusting, and stacking. Additional deformation occurred along the steep boundaries of the orogenic belt through interaction with shear zones and gravitational effects. In the second stage, this linear mountain belt was disrupted by strike-slip faulting to produce the presently observed morphology. Several models describing this second stage have been presented above (Figure 13). The first two suggest that Maxwell Montes underwent large-scale strike-slip motion while situated at its present location, either with or without large-scale rotation of the CSDs. A third model involves lateral transport of the entire mountain range within two converging shear zones. A combination of this last model with some rotation of the mountain belt during transport can account for the majority of features observed including the morphology, topography, and sense of shear along both the CSDs and the shear zones. Based on our study of Maxwell Montes and the three models, it is possible to determine the relative ages of a number of structures and features in and around Maxwell Montes, so that a more detailed deformational history may be recognized. Figure 14 shows a summary of this multistage evolution.

Formation of proto-Maxwell Montes. The first stage (Figure 14*a*) involves the formation of the Akna Montes-like proto-Maxwell Montes as a linear mountain belt. Compressional stress oriented at N70°E formed an orogenic belt that was 300 km wide and 1200 km long. By direct analogy with Akna Montes we suggest that the banded units and dissected terrain of Maxwell Montes may have formed synchronously as compressional ridges and troughs, with a continuous, linear boundary between the two units. The continuous ridges of the banded units would represent the deformational front of the mountain range, with the less continuous ridges of the dissected terrain representing slightly more complex hinterland deformation. In this scenario, the deformation in the dissected terrain may be similar to that behind the Himalayan front in the Tibetan Plateau, which is characterized by compressional ridges and troughs often disrupted by later stage extensional graben [*Molnar and Tapponier*, 1978]. Alternatively, the more disrupted nature of the dissected terrain could be the result of continued imbrication and suturing of crustal blocks beyond the banded units, as *Head* [1990] has interpreted the ridged and domed unit in Freyja Montes. However, this suture model seems less likely at Maxwell because the dissected terrain does not contain any obvious linear troughs that could represent the location of crustal underthrusting. Regardless of the specific style of orogeny, the creation of proto-Maxwell Montes as a long, linear mountain belt is the initial stage in its evolution.

Cleopatra and associated deposits. Following the creation of proto-Maxwell Montes, our reconstruction suggests that the dissected terrain was a single, contiguous unit running north-south across the entire eastern slope of proto-Maxwell Montes, before being overlain by the bright terrain associated with Cleopatra Patera (Figure 14*b*). *Peterfreund et al.* [1984] have suggested that Cleopatra formed before the ridges. They based this argument on the observed disruption of the rim of this structure and what they described as the deflection of large ridges around Cleopatra. This interpretation was made without the benefit of the Venera data sets, however, which were unavailable at that time. Although it is true that the rim of Cleopatra is somewhat disrupted (Figure 2), if Cleopatra were present before the initial stage of N70°E compression, then it would be elongated in a NW-SE direction consistent with the shortening associated with the formation of the ridges. Such an elongation is not observed. Disruption of the rim of Cleopatra could instead be due to structural control by the preexisting ridge pattern. In addition, we attribute the superficial deflection of large ridges about Cleopatra to the arcuate nature of the mountain range (Figure 11). Finally, the Venera image (Figure 2*b*) reveals that small ridges to the immediate south of Cleopatra in the dissected terrain are not deflected at all. It is unreasonable to suggest that ridges over 100 km away could be deflected while others within 50 km were not. Therefore we believe that the weight of the evidence supports the interpretation that the Cleopatra structure was created after ridge formation, but prior to strike-slip faulting. Since creation of the dissected terrain occurs synchronously with ridge formation, then Cleopatra must have been superposed on the dissected terrain unit. This superposition relationship suggests that formation of Cleopatra Patera followed the creation of the dissected terrain. Whether Cleopatra originated as an impact crater [*Basilevsky et al.*, 1986] or as a volcanic caldera [*Schaber et al.*, 1987*a*] cannot be determined from our present study, but high-resolution images to be obtained by the Magellan spacecraft should help resolve this issue.

Strike-slip faulting and lateral transport. The next phase in the development of Maxwell Montes was the creation of strike-slip faults (CSDs) and offset along these faults (Figure 14*c*). The exact reason for the change in style of deformation is uncertain, but could be attributed to any of the three models discussed above and illustrated in Figure 13: (1) regional NNW-SSE compression of the mountain belt resulting in the formation of the CSDs and strike-slip faulting along them but

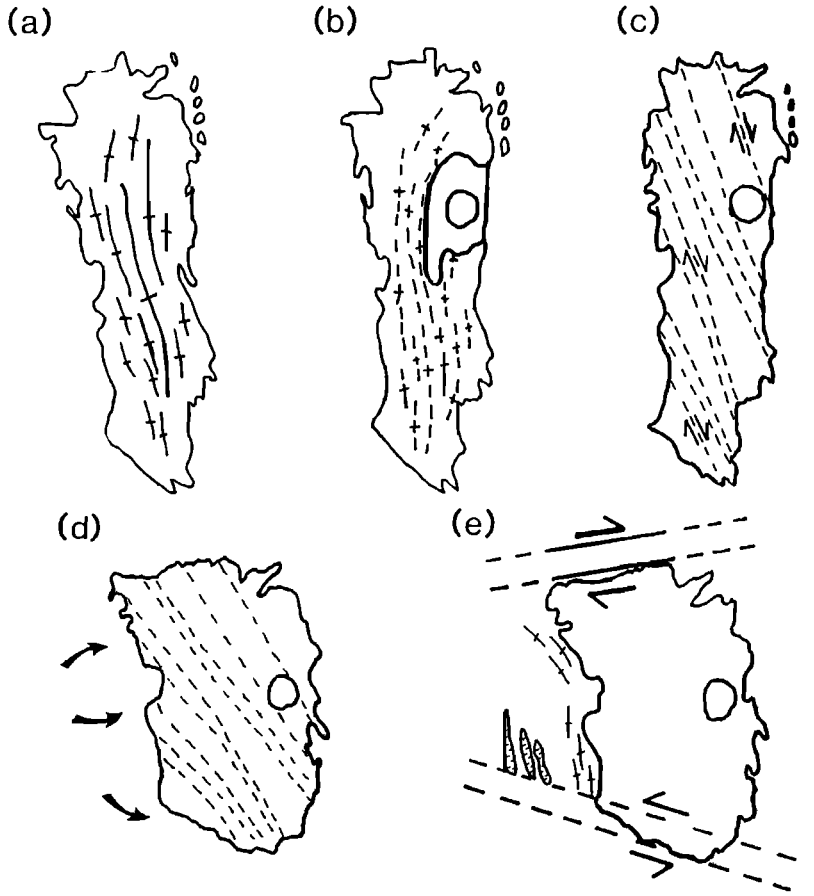

Fig. 14 Summary sketches of the sequence of events in the evolution of Maxwell Montes. (*a*) Initial formation of proto-Maxwell Montes as an Akna-like linear mountain belt. Simultaneous formation of dissected terrain. (*b*) Formation of Cleopatra Patera and emplacement of bright terrain. (*c*) Creation of, and strike-slip movement along, the cross-strike discontinuities. (*d*) Plains flooding to west and south. (*e*) Movement along shear zones and formation of extensional troughs and compressional ridges to the west of Maxwell.

without large-scale rotation of the mountain range; (2) regional N-S compression, CSD formation and offset, and large-scale counterclockwise rotation of the entire mountain belt; or (3) E-W lateral transport of proto-Maxwell Montes within two converging shear zones, resulting in NNW-SSE compression leading to CSD formation and offset. The amount of lateral transport is related to the amount of large-scale rotation of the mountain range during strike-slip offset. We favor a model involving some lateral transport accompanied by large-scale rotation.

Regardless of its specific cause, the strike-slip faulting would have produced the offset of large-scale linear and curvilinear features such as ridges, valleys, unit boundaries, and topographic contours (Figure 11). It is during this phase that Maxwell Montes underwent extensive large-scale deformation until it had attained close to its present configuration.

Late stage deformation. The final events in the evolution of Maxwell Montes include the embayment of western and southern Maxwell by volcanic flows on Lakshmi Planum (Figure 14*d*). These flow units were then disrupted to form the compressional ridges of the dark bands unit at the foot of Maxwell and the extensional troughs farther west, along with some deformation along the northern and southern shear zones (Figure 14*e*). Although one would expect large-scale gravitational relaxation of such a high mountain range, we find no obvious evidence for extensional deformation perpendicular to the strike of the mountain belt in the high central region. Instead, we note some potential N-S extension only on the northern and southern flanks in the form of short linear troughs. These troughs do not appear to accommodate great strain and may, in fact, be more closely related to strike-slip deformation associated with the north and south bounding shear zones. The lack of obvious extensional features in central Maxwell, the highest region on the planet, and the potentially minimal extension represented by the troughs on the north and south slopes suggests that Maxwell Montes may still be undergoing some NNW-SSE oriented compression, preventing large-scale gravitational relaxation from taking place. Alternatively, the compressional deformation of Maxwell Montes may have ceased recently enough that gravitational relaxation has not yet had time to produce recognizable features. If the viscosity of the lithosphere is low, then this time would be relatively short.

CONCLUSIONS

On the basis of our analysis we draw the following conclusions regarding the evolution of Maxwell Montes and the nature of tectonics on Venus:

Style of deformation. The majority of ridges and troughs in all units are compressional in origin. The transitional units show evidence of multiple deformation which can be interpreted as an initial stage of compression, followed by an additional deformation due to interactions with the shear zones and gravitational deformation. The dissected terrain also underwent an initial compressional event, followed by a second stage of deformation related to the strike-slip faulting. The deposits of the bright terrain unit were the result of a late-stage event, since they are not deformed by tectonic processes that affected the other units. They may represent either volcanic flows or impact ejecta and melt. The other smooth units occur in local lows and may represent smooth volcanic flows since they are radar-dark, although they could have a low radar cross section due to their low altitude. Overall, we find that Maxwell Montes is a compressional orogenic belt, characterized by parallel ridges resulting from the horizontal convergence of crustal materials toward Lakshmi Planum from the east-northeast.

Cross-strike discontinuitites. Nine long, linear cross-strike discontinuities are observed to cut across the structure of Maxwell Montes, disrupting ridges and unit boundaries, and dividing the mountain range into 10 crustal domains. These cross-strike discontinuities represent strike-slip faults along which the crustal domains have been offset in a right-lateral sense from 10 to 125 km.

Large-scale evolution. Retrodeformation of crustal domains to their pre-strike-slip form creates a linear mountain belt remarkably similar to the Akna Montes mountain belt, suggesting that Akna Montes may represent the initial, relatively simple form of compressional orogenic belts on Venus. We have presented three models to account for the evolution of Maxwell Montes from this simple orogenic stage to the present configuration (Figure 13). The first two models suggest that strike-slip faulting occurred while the mountain belt remained in place, either with or without large-scale rotation, while the third model suggests that strike-slip faulting was accompanied by large-scale transport of the mountain range from east to west within converging shear zones without large-scale rotation. We favor a combination of the last two models (Figures 13*b* and 13*c*), in which some east-west lateral transport was accompanied by large-scale counterclockwise rotation of the range within the converging shear zones. This model can account for the observed morphology, topography, and sense of offset on the CSDs and shear zones.

Sequence of deformation. A sequence of deformation for Maxwell Montes that can account for the observations is as follows:

1. Formation of an Akna Montes-like long linear mountain belt between two converging shear zones, accompanied by formation of the dissected terrain. This mountain belt had up to 11 km of elevation.
2. Creation of the circular stucture Cleopatra, and emplacement of bright terrain associated with this structure.
3. Creation of, and movement along, strike-slip faults, resulting in the present configuration of Maxwell Montes.
4. Plains flooding to the west and south of Maxwell Montes.
5. Further deformation in the plains, creating folds in volcanic units to the immediate west of Maxwell Montes and arcuate, extensional troughs farther west.

Age of Maxwell Montes. The lack of obvious extensional features along the crest of Maxwell Montes indicates that gravitational relaxation has not significantly affected the mountain range as a whole, and that Maxwell Montes is a young feature (< 200-600 m.y. old) which may still be undergoing deformation.

Finally, from this study, one can conclude that horizontal motion of crustal materials in the form of large-scale compressional folding, strike-slip faulting, and shear represent fundamental aspects of the tectonics of Ishtar Terra and Venus in contrast to the smaller, one-plate planets, Mars, Mercury, and Moon.

QUESTIONS FOR MAGELLAN

In August 1990, the Magellan spacecraft will arrive at Venus and begin to take radar images of the Venusian surface at resolutions of better than 300 m. The data returned from this mission will enable us to test many of the observations and interpretations presented here and to distinguish more confidently between the three models for the second stage of the evolution of Maxwell Montes. Of primary importance will be the further defintion and characterization of the cross-strike discontinuities and features associated with them. Similarly, a better characterization of the shear zones that bound Maxwell Montes on the north and south will provide further insight into the evolution of Maxwell Montes. The high-resolution images should also enable us to determine if normal faulting has occurred near the crest of Maxwell Montes and therefore constrain the stress regime across the belt. Other features related to gravitational relaxation also might be observed in and around the mountain belt. In addition, the nature of Cleopatra and the deposits associated with it should further enhance our understanding of this region. Finally, the charcteristics of the dark bands unit west of Maxwell should provide insight into the process of orogeny on Venus, as we interpret this as the location of incipient mountain building.

Acknowledgments. The financial support of National Aeronautics and Space Administration grants NGR-40-002-116 and NAGW-713, from the Planetary Geology and Geophysics Program of the Solar System Exploration Division, Office of Space Science and Applications, is gratefully acknowledged. D.B.C. gratefully acknowledges the support of the National Aeronautics and Space Administration, Planetary Astronomy Program. We also thank the staff of the Arecibo Observatory for their assistance in data collection; the National Astronomy and Ionosphere Center is operated by Cornell University under a cooperative agreement with the National Science Foundation and with support from the National Aeronautics and Space Administration. Mary Ellen Murphy, Angel Hilliard, and Peter Neivert assisted greatly in the preparation of the manuscript. Particular thanks are extended to Bill McKinnon, Maria Zuber, an anonymous reviewer, Jason Morgan, Ted Maxwell, and Bob Grimm for helpful reviews. We are also grateful to John Harmon, Alice Hine, Wendy Hale Ehrlich, Larry Crumpler, Scott Murchie, Ellen Stofan, Duane Bindschadler, and John Mustard for many helpful discussions related to this paper,and for reviews of the manuscript.

REFERENCES

Armijo, R., P. Tapponnier, J.L. Mercier, and H. Tong-Lin, Quaternary extension in southern Tibet: Field observations and tectonic implications, *J. Geophys. Res.*, *91*, 13,803-13,872, 1986.

Barsukov, V.L., et al., The geology and geomorphology of the Venus surface as revealed by the radar images obtained by Veneras 15 and 16, *Proc. Lunar Planet. Sci. Conf. 16th*, Part 2, *J. Geophys. Res.*, *91*, suppl., D378-D398, 1986.

Basilevsky, A.T., A.A. Pronin, L.B. Ronca, V.P. Kryuchkov, A.L. Sukhanov, and M.S. Markov, Styles of tectonic deformation on Venus: Analysis of Veneras 15 and 16 data, *Proc. Lunar Planet. Sci.*

Conf. 16th, Part 2, *J. Geophys. Res.*, *91*, suppl. D399-D411, 1986.

Basilevsky, A.T., B.A. Ivanov, G.A. Burba, I.M. Chernaya, V.P. Kryuchkov, O.V. Nikolaeva, D.B. Campbell, and L.B. Ronca, Impact craters on Venus: A continuation of the analysis of data from the Venera 15 and 16 spacecraft, *J. Geophys. Res.*, *92*, 12,869-12,901, 1987.

Bolt, B.A., C. Lomnitz, and T.V. McEvilly, Seismological evidence on the tectonics of central and northern California and the Mendocino Escarpment, *Bull. Seismol. Soc. Am.*, *58*, 1725-1767, 1968.

Burchfiel, B.C. and L.H. Royden, North-south extension within the convergent Himalayan region, *Geology*, *13*, 679-682, 1985.

Burke, K., C. Sengor, and P. Francis, Maxwell Montes in Ishtar–A collisional plateau on Venus? (abstract), Lunar Planet. Sci. XV, 104-105, 1984.

Campbell, D.B., J.W. Head, J.K. Harmon, A.A. Hine, Venus: Identification of banded terrain in the mountains of Ishtar Terra, *Science*, *221*, 644-647, 1983.

Crowell, J.C., and V.R. Ramirez, Late Cenozoic faults in southeastern California, in *Tectonics of the Juncture Between the San Andreas Fault System and the Salton Trough, Southeastern California - A Guidebook*, edited by J.C. Crowell, and A.G. Sylvester, pp. 27-39, Geological Society of America, Boulder, Colo., 1979.

Crumpler, L.S., J.W. Head, and D.B. Campbell, Orogenic belts on Venus, *Geology*, *14*, 1031-1034, 1986.

Crumpler, L.S., J.W. Head, and J.K. Harmon, Regional linear cross-strike discontinuities in western Aphrodite Terra, Venus, *Geophys. Res. Lett.*, *14*, 607-610, 1987.

Dalmayrac, B., and P. Molnar, Parallel thrust and normal faulting in Peru and constraints on the state of stress, *Earth Planet. Sci. Lett.*, *55*, 473-481, 1981.

Ford, J. P., Seasat orbital imagery for geological mapping: Tennessee-Kentucky-Virginia, *Am. Assoc. Pet. Geol. Bull.*, *64*, 2064-2094, 1980.

Garfunkel, Z., and H. Ron, Block rotation and deformation by strike-slip faults, 2, The properties of a type of macroscopic discontinuous deformation, *J. Geophys. Res.*, *90*, 8589-8602, 1985.

Garvin, J.B., J.W. Head, M.T. Zuber, and P. Helfenstein, Venus: The nature of the surface from Venera panoramas, *J. Geophys. Res.*, *89*, 3381-3399, 1984.

Hagfors, T., Backscattering from an undulating surface with application to radar returns from the Moon, *J. Geophys. Res.*, *69*, 3775-3784, 1964.

Hagfors, T., Remote probing of the Moon by microwave and infrared emissions and radar, *Radio Sci.*, *5*, 189-227, 1970.

Harding, T.P., Petroleum traps associated with wrench faults, *Am. Assoc. Pet. Geol. Bull.*, *58*, 1290-1304, 1974.

Harding, T.P., Tectonic significance and hydrocarbon trapping consequences of sequential folding synchronous with San Andreas faulting, San Joaquin Valley, California, *Am. Assoc. Pet. Geol. Bull.*, *60*, 356-378, 1976.

Head, J.W., Ishtar Terra, Venus: A simple model of large scale tectonic convergence, possible thickening, and possible delamination (abstract), *Lunar Planet. Sci., XVII*, 323-324, 1986.

Head, J.W., Formation of mountain belts on Venus: Evidence for large-scale convergence, underthrusting, and crustal imbrication in Freyja Montes, Ishtar Terra, *Geology*, *18*, 99-102, 1990.

Head, J.W., and L.S. Crumpler, Evidence for divergent plate boundary characteristics and crustal spreading: Aphrodite Terra, *Science*, *238*, 1380-1385, 1987.

Ivanov, B.A., A.T. Basilevsky, V.P. Kryuchkov, and I.M. Chernaya, Impact craters of Venus: Analysis of Venera 15 and 16 data, *Proc. Lunar Planet. Sci. Conf. 16th*, Part 2, *J. Geophys. Res.*, *91*, suppl., D413-D430, 1986.

Kozak, R.C., and G.G. Schaber, New evidence for global tectonic zones on Venus, *Geophys. Res. Lett.*, *16*, 175-178, 1989.

Magee, K.P., and J.W. Head, Lakshmi Planum: A distinctive highland volcanic province (abstract), *Lunar Planet. Sci., XIX*, 713-714, 1988.

Masursky, H., E. Eliason, P.G. Ford, G.E. McGill, G.H. Pettengill, G.G. Schaber, and G. Schubert, Pioneer Venus radar results: Geology from images and altimetry, *J. Geophys. Res.*, *85*, 8232-8260, 1980.

Molnar, P., and P. Tapponier, Active tectonics of Tibet, *J. Geophys. Res.*, *83*, 5361-5375, 1978.

Peterfreund, A.R., J.W. Head, R.A.F. Grieve, and D.B. Campbell, Cleopatra Patera, a circular structure in Maxwell Montes, Venus; Volcanic or impact? (abstract), *Lunar Planet. Sci., XV*, 641-642, 1984.

Pettengill, G.H., E. Eliason, P.G. Ford, G.B. Loriot, H. Masursky, and G.E. McGill, Pioneer-Venus radar results: Altimetry and surface properties, *J. Geophys. Res.*, *85*, 8261-8270, 1980.

Pettengill, G.H., P.G. Ford, and S. Nozette, Venus: Global surface radar reflectivity, *Science*, *217*, 640-642, 1982.

Pronin, A.A., et al., Geological-Morphological description of the Lakshmi Planum (in Russian), *Astron. Vestn., XX(2)*, 83-98, 1986.

Ronca, L.B., and A.T. Basilevsky, Maxwell Montes and Thessera Fortuna: A study of Venera 15 and 16 radar images, *Earth Moon and Planets*, *36*, 23-39, 1986.

Rzhiga, O.N., Venera-15 and -16 spacecraft: Images and maps of Venus, *Adv. Space Res.*, *7*, (12)269-(12)278, 1987.

Schaber, G.G., R.C. Kozak, and H. Masursky, Cleopatra Patera on Venus: Venera 15/16 evidence for a volcanic origin, *Geophys. Res. Lett.*, *14*, 41-44, 1987*a*.

Schaber, G.G., E.M. Shoemaker, and R.C. Kozak, The surface age of Venus: Use of terrestrial cratering record, *Astron. Vestn., XXI(2)*, 144-151, 1987*b*.

Sharpton, V.L., and J.W. Head, A comparison of the regional slope characteristics of Venus and Earth: Implications for geologic processes on Venus, *J. Geophys. Res.*, *91*, 7545-7554, 1986.

Solomon, S.C., and J.W. Head, Venus banded terrain: Tectonic models for band formation and their relationship to lithospheric thermal structure, *J. Geophys. Res.*, *89*, 6885-6897, 1984.

Solomon, S.C., S.K. Stephens, and J.W. Head, On Venus impact basins: Viscous relaxation of topographic relief, *J. Geophys. Res.*, *87*, 7763-7771, 1982.

Stephens, S.K., S.C. Solomon, and J.W. Head, On the age of Venus highland topography: Constraints from the viscous relaxation of relief (abstract), *Lunar Planet. Sci., XIV*, 747-748, 1983.

Stoddard, P.R., A kinematic model for the evolution of the Gorda plate, *J. Geophys. Res.*, *92*, 11,524-11,532, 1987.

Sylvester, A.G., Wrench fault tectonics - Introduction, in *Wrench Fault Tectonics*, edited by A.G. Sylvester, pp. v-ix, American Association of Petroleum Geologists, Tulsa, Okla.,1984.

Tapponnier, P., G. Peltzer, Y.A. Le Dain, R. Armijo, and P. Cobbold, Propagating extrusion tectonics in Asia: New insights from simple experiments with plasticine, *Geology*, *10*, 611-616, 1982.

Vorder Bruegge, R.W., The geomorphology and tectonic evolution of Maxwell Montes, Venus, M. S. thesis, 81pp., Brown Univ., Providence, R.I., 1987.

Vorder Bruegge, R.W., and J.W. Head, Multi-stage tectonic evolution of eastern Ishtar Terra, Venus (abstract), *Lunar Planet. Sci., XX*, 1162-1163, 1989*a*.

Vorder Bruegge, R.W., and J.W. Head, Fortuna Tessera, Venus: Evidence of horizontal convergence and crustal thickening, *Geophys. Res. Lett.*, *16*, 699-702, 1989*b*.

Weertman, J., Height of mountains on Venus and the creep properties of rock, *Phys. Earth Planet. Inter.*, *19*, 197-207, 1979.

Wheeler, R.L., Cross-strike discontinuities: Possible exploration tool for natural gas in Appalachian Overthrust belt, *Am. Assoc. Pet. Geol. Bull.*, *64*, 2166-2178, 1980.

Wilson, D.S., A kinematic model for the Gorda deformation zone as a diffuse southern boundary of the Juan de Fuca Plate, *J. Geophys. Res.*, *91*, 10,259-10,270, 1986.

Zhao, W.L., and W.J. Morgan, Uplift of Tibetan Plateau, *Tectonics*, *4*, 359-369, 1985.

D.B. Campbell, National Astronomy and Ionosphere Center, Cornell University, Space Sciences Bldg., Ithaca, NY 14853

J.W. Head and R.W. Vorder Bruegge, Department of Geological Sciences, Brown University, Box 1846, Providence, RI 02912

(Received January 6, 1989;
revised November 27, 1989;
accepted December 5, 1989)